



An experimental investigation on hydrogen fuel injection in intake port and manifold with different EGR rates

N.Saravanan¹, G.Nagarajan²

¹ Manager, ERC Engines, Tata Motors Ltd., Pimpri, Pune-411019, India.

² Department of Mechanical Engineering, College of Engineering, Guindy, Anna University Chennai, Chennai 600025, India.

Abstract

In the present investigation hydrogen was used in a diesel engine in the dual fuel mode using diesel as an ignition source. In order to have a precise control of hydrogen flow and to avoid the backfire and pre-ignition problems hydrogen was injected into the intake system. Experiments were conducted to determine the optimized injection timing, injection duration and injection quantity of the fuel in manifold and port injected hydrogen-operated engine using diesel as ignition source for hydrogen operation. From the results it was observed that in manifold injection technique the optimized condition was start of injection at gas exchange top dead centre (GTDC) with injection duration of 30° crank angle (CA) with hydrogen flow rate of 7.5 litres/min. In port injection technique, the optimized condition was start of injection at 5° before gas exchange top dead centre (5°BGTDC) with injection duration of 30° CA with hydrogen flow rate of 7.5 litres/min. With the above optimized timings of port and manifold injection it was observed that brake thermal efficiency in port injection increases by 13 % and 16 % in manifold injection at 75 % load. However at full load the brake thermal efficiency decreases by 1 % in port injection and 8 % in manifold injection. A reduction in NO_x emission by 4 times is observed in port injection and 7 times in manifold injection at full load. At 75 % load the NO_x emission reduces by 3 times in both port injection and manifold injection. Smoke emission increases with increase in EGR percentage. The smoke increases by 36 % at full load in port injection and by 44 % in manifold injection. At 75 % load the smoke emission reduces by 13 % in port injection and 9 % in manifold injection. In both the port injection and manifold injection ignition delay was 12° or 1.33 ms while for diesel it was 11° or 1.22 ms. Port injection system with diesel as ignition source operates smoothly and shows improved performance and emit lesser pollution than diesel.

Copyright © 2010 International Energy and Environment Foundation - All rights reserved.

Keywords: Hydrogen injection, Performance, Emission, Dual fuel combustion, EGR.

1. Introduction

Diesel engines are the main prime movers for public transportation vehicles, stationary power generation units and for agricultural applications. But diesel engines are found to emit more NO_x and smoke emissions in addition to its rapid depletion. Hence it is very important to find a best alternate fuel, which can fully or partially replace diesel which emits fewer pollutants to the atmosphere from diesel engines [1]. In this regard hydrogen is receiving considerable attention as an alternative source of energy to replace the rapidly depleting petroleum resources [2]. Its clean burning characteristics provide a strong

incentive to study its utilization as a possible alternate fuel. While electrochemically reacting hydrogen in fuel cell was considered to be the cleanest and most efficient means of using hydrogen, it was believed by many to be a technology of the distant future [3, 4]. Currently fuel cell technology is expensive and bulky. In the near term, the use of hydrogen in internal combustion engine may be feasible as a low cost technology to reduce emissions [5, 6]. Hydrogen can be adapted in both SI and CI engines. In SI engine hydrogen can be used as a sole fuel, but in the case of CI engine dual fuelling technique is used. The concept of using hydrogen as an alternative to diesel fuel in C.I engines was a recent one. As the self-ignition temperature of hydrogen (858 K) is higher than diesel (453 K), hydrogen cannot be ignited by compression. Hence it requires the use of external ignition source like a spark plug or a glow plug.

One of the alternative methods is to use diesel as a pilot fuel for ignition purpose or by using ignition improvers like DEE. The methods of using hydrogen in C.I. engines are;

1. Hydrogen enrichment in air
2. Hydrogen injection in the intake system
3. In cylinder injection

Hydrogen substitution by 10-20 % of energy share in diesel reduces substantially the smoke, particulate and soot emissions. Hydrogen powered I.C. engines produces more or similar power compared to diesel. The problems of preignition and backfire are less severe and knock can be eliminated compared to spark ignited engines that make the hydrogen usage to be safer in CI mode rather than SI mode.

The Ministry of Non-conventional Energy Sources with an annual operating budget of US \$ 100 million has been extensively supporting hydrogen and fuel cell research at many of India's top universities and public research laboratories. Researchers have been successful in the biological production of hydrogen from organic effluents and a large-scale bioreactor of 12.5 m³ capacity is being developed in India [7]. Efforts are also underway to utilize significant amounts of hydrogen produced as a byproduct in many industries such as the chlor-alkali industry, which currently has no applications. In 2003 India joined the International partnership for the hydrogen economy a move that will provide impetus to collaborative research and funding opportunities. The US Department of Energy and US based ECD Ovonic, Inc have already launched a collaborative effort with Indian auto manufacturer to launch a hydrogen powered three wheeler with a grant of US \$ 5,00,000 from the US agency for international development. The Ministry of Non-Conventional Energy sources have set up a National Hydrogen Energy Board (NHEB) under the chairmanship of Mr. Ratan Tata for the development of national hydrogen energy road map. NHEB has also proposed to launch 1000 hydrogen vehicles by 2009 including 500 small three wheelers, 300 heavy vehicles and 200 buses [8].

Several works have been done earlier on hydrogen. Das [9] observed that hydrogen engine develops lesser power mainly due to its low volumetric energy density. Various fuel induction techniques such as carburation, continuous manifold injection, timed manifold injection (TMI) and direct cylinder injection were investigated and (TMI) was adopted by the author since it gave higher thermal efficiency and eliminated undesirable combustion. It was observed that under stoichiometric condition, hydrogen occupies 29.6 % by volume whereas gasoline-air mixture occupies only about 2 % by volume. Yi et al [10] have carried out work on both port injection and in-cylinder injection hydrogen fuel supply systems. Their results indicated that the thermal efficiency of the intake port injection was higher than in-cylinder injection at all equivalence ratios. In order to minimize the possibility of flashback occurrence, the injection timing of the hydrogen injection was fixed in coordination with the intake valve opening timing.

Hydrogen used in the dual fuel mode with diesel by Masood et al [11] showed the highest brake thermal efficiency of 30 % at a compression ratio of 24.5. Lee et al [11] studied the performance of dual injection hydrogen fueled engine by using in-cylinder injection and external fuel injection techniques. An increase in thermal efficiency by about 22 % was noted for dual injection at low loads and 5 % at high loads compared to direct injection. Jong T. Lee et al [12] suggested that in dual injection, the stability and maximum power could be obtained in direct injection of hydrogen. However it was observed that the maximum efficiency could be obtained by external mixture formation in hydrogen engine.

The most important advantage of hydrogen fueled engine is that they emit fewer pollutants than comparable diesel fueled engine. In hydrogen fueled engine, the principal exhaust products are water vapor and NO_x. Emissions such as HC, CO, CO₂, SO_x and smoke are either not observed or are very much lower than those of diesel engine [13]. Small amount of hydrogen peroxide may be found in the exhaust of the hydrogen-operated engine [14]. Unburnt hydrogen may also come out of the engine, but

this is not a problem since hydrogen is non-toxic and does not involve in any smog producing reaction. NO_x are the most significant emission of concern from a hydrogen engine [15]. NO_x have an adverse effect on air quality through the formation of ozone or acid rain. In order to reduce the NO_x , in the present work exhaust gas recirculation (EGR) technique was adopted. Exhaust gases from the engine were by-passed, regulated and cooled by using a counter flow type heat exchanger in the EGR unit. The flow rate of EGR cooling water was varied in such a way that the cooled exhaust gas temperature was maintained around 30°C . The cooled exhaust gas was allowed to pass through a filtering device to remove the soot and particulate matter from the exhaust gas. The EGR flow rate was determined by measuring the CO_2 concentration in the exhaust gas [15]. The EGR percentage was calculated from the ratio of CO_2 concentration present in the intake manifold to the CO_2 concentration present in the exhaust gas. The flow rate of EGR was increased until the necessary CO_2 concentration in the intake manifold was attained. The schematic view of the EGR unit is shown in Figure 1.

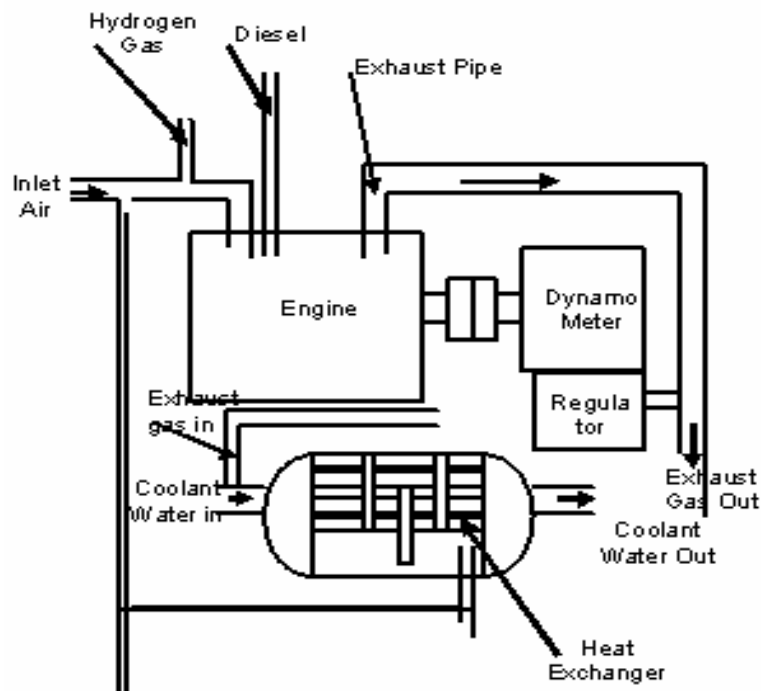


Figure 1. Schematic view of the EGR unit

2. Safety arrangements

Hydrogen fuel is often associated with either the Hindenburg or Challenger disasters or even the hydrogen bomb. However other fuels such as gasoline and natural gas pose similar dangers. Hydrogen actually has a good overall safety record due to strict adherence to regulations and procedures, good training for the persons who handle hydrogen [16]. In order to have the overall safety the safety devices given below and some safety measures have been taken for hydrogen operation.

A special, effective hydrogen sensor was used to monitor the hydrogen gas in the operating environment and also used to sense any leak of hydrogen through the pipeline during the operation of the engine. The sensor works on the principle of electrochemical reaction. Hydrogen has the highest diffusivity characteristics, of about 3-8 times faster in air. Any hydrogen leakage will result in quicker dispersion in air compared to that of hydrocarbon dispersion. Hence it will not form any cloud of hydrogen vapour in the working space [10]. Blowers were also made available to disperse the hydrogen gas if present in the environment and proper ventilation was provided during engine operation. The hydrogen cylinders were also stored away from the working environment. The crankcase for the hydrogen-operated engine was properly ventilated to avoid ignition from taking place inside due to blow by gases. The clouds of gases collected in the crankcase were removed from the rocker arm holes and were vented into the atmosphere. The hydrogen present in the rocker arm assembly was found to be around 40-80 ppm during hydrogen operation [17]. Flame arrestor was used to suppress explosion inside the hydrogen cylinder. The flame

arrestor consists of a tank partly filled with water with a fine wire mesh to prevent the flame propagation beyond the wire mesh. The flame also gets quenched while reaching the water surface in case of any backfire. A non-return line was provided to prevent the reverse flow of hydrogen into the system. Such a possibility of reverse flow can occur sometimes in hydrogen – injected engine, particularly in the later part of injection duration. Flow indicator was used to visualise the flow of hydrogen during engine operations. As the hydrogen was allowed to pass through a glass tube containing water, bubbles were formed during hydrogen flow, which clearly showed the flow of hydrogen.

3. Experimental setup

In the present work, single cylinder water cooled DI diesel engine having a rated speed of 1500 rpm developing 3.7 kW was converted to operate on dual fuel mode with hydrogen adopting timed manifold injection (TMI) and timed port injection technique (TPI). The methodology of hydrogen injection is shown in Figure 2. An electronic control system was used to control the injection timings of hydrogen [18]. The experimental work includes of development of hydrogen injection setup for TMI. The performance and emission characteristics of the modified system are compared with the baseline diesel.

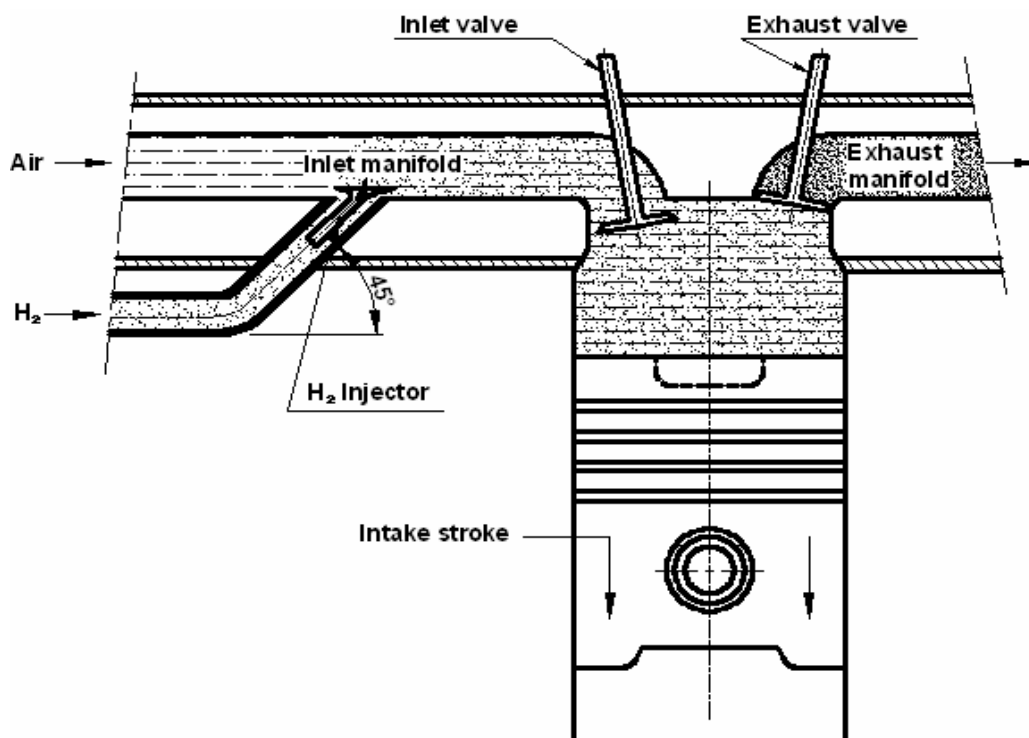


Figure 2. Methodology of hydrogen enrichment in air

Hydrogen was stored in a high-pressure storage tank at a pressure of 150 bar having a capacity of 7 cubic meter (0.5 kg) of hydrogen. A double stage pressure regulator was used to control the hydrogen from the cylinder. The pressure was reduced to the range of 1-4 bar based on the flow requirements. The hydrogen from the pressure regulator was passed through a shut off valve, which can be closed if any backfire results in the fuel pipeline. The hydrogen after passing through the shut off valve was allowed to pass through the digital mass flow controller (DFC). The DFC precisely measures the flow rate of hydrogen in standard liters per minute (SLPM). Since the hydrogen flow to the injector should be free from any impurities the hydrogen was passed through a filtering device. The hydrogen from the filter was passed to a flame arrestor. The flame arrestor acted as a non-return valve and also it as a visible indicator for hydrogen flow [18]. The hydrogen from the flame arrestor was then passed to the flame trap, which consisted of wire mesh. The wire mesh will prevent the penetration of flame to the hydrogen cylinder. The flame arrestor also acted as a non-return valve (NRV). The flame arrestor consisted of a bursting diaphragm, which punctures of when the pressure built on the system exceeds 10 bar during backfire conditions. Figure 3 shows the schematic view of the experimental setup. Table 1 shows the hydrogen injector specifications.

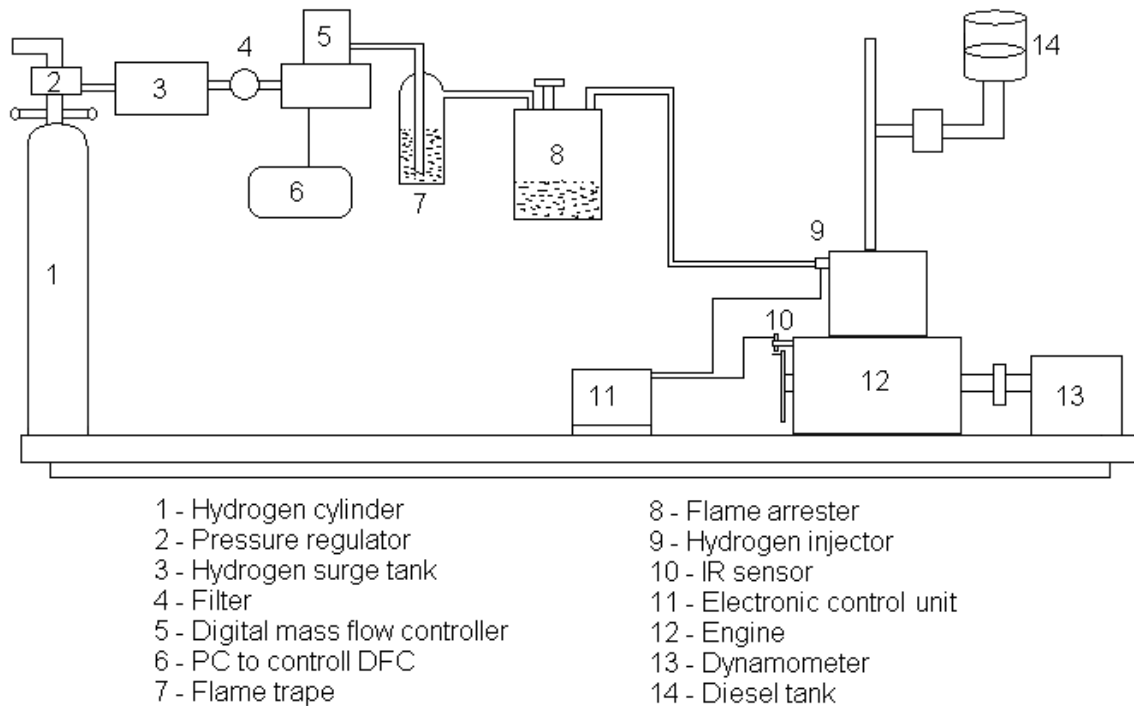


Figure 3. Schematic view of the experimental setup

Table 1. Hydrogen fuel injector specifications

Make	Quantum technologies
Supply Voltage	8 – 16 Volts
Peak Current	4 Amps
Holding Current	1 Amp
Flow Capacity	0.8 g /s @ 483-552 kPa
Working Pressure	103 – 552 kPa
Durability	>500 Million cycles
Dynamic range	12:1 Typical
Length	79.8 mm
Diameter (Max)	24.5 mm (Excl connector)
Resistance	2.05 +/-0.25Ω at 20°C
Inductance	3.98 +/- 0.3 mH at 1000Hz typical

The hydrogen from the flame trap was passed to the 2-way valve. One end of the two-way valve was connected to the pipeline and it was kept away from the working area. This was done to remove the excess hydrogen in the fuel line during the engine shutoff time. The other end of the two-way valve was connected to a selector switch, which will permit the supply of hydrogen to either the port fuel injector or the manifold injector. The port injector was placed in the engine head 13 mm above the intake valve and the manifold injector was placed at a distance of 100 mm away from the engine head in the intake manifold. A Quantum make gas injector was used. An electronic control unit (ECU) controlled the injector opening timing and duration. An infrared detector was used to give the signal to the ECU for the injector opening. Based on the preset timing and duration the injector was opened for injection and closed after injection. The injection timing and injection duration was varied within the specified range by using a knob. The power supply for opening the injector was 4A and for holding the armature to inject the fuel was 1A. Figure 4 shows the peak and holding current of the hydrogen injector. Based on the

preset timing the hydrogen flow was taking place and the flow was controlled by using the pressure regulator and also by using the digital mass flow controller. Figure 5 shows the hydrogen injector positioning on the cylinder head. Table 2 shows the properties of hydrogen in comparison with diesel.

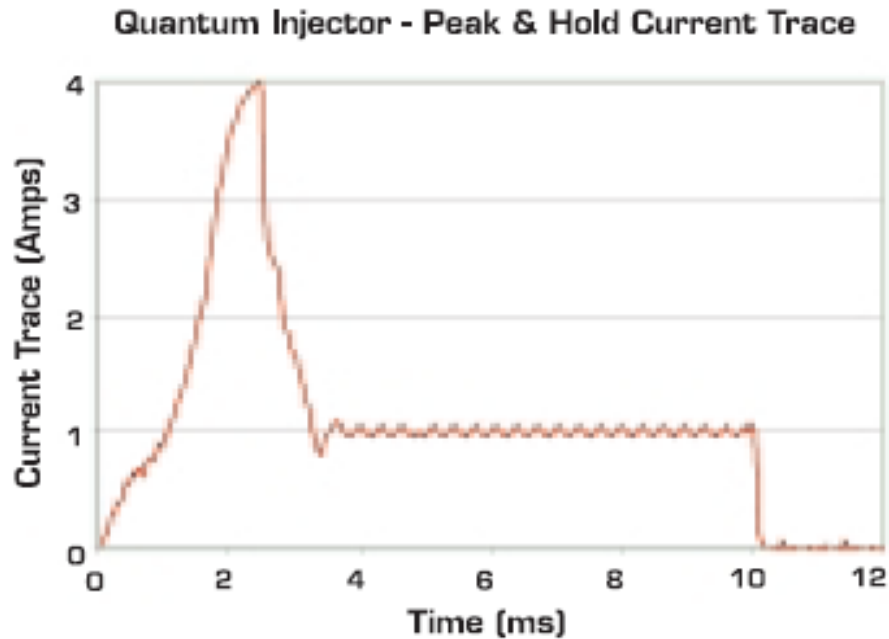


Figure 4. Peak and hold current for the hydrogen injector

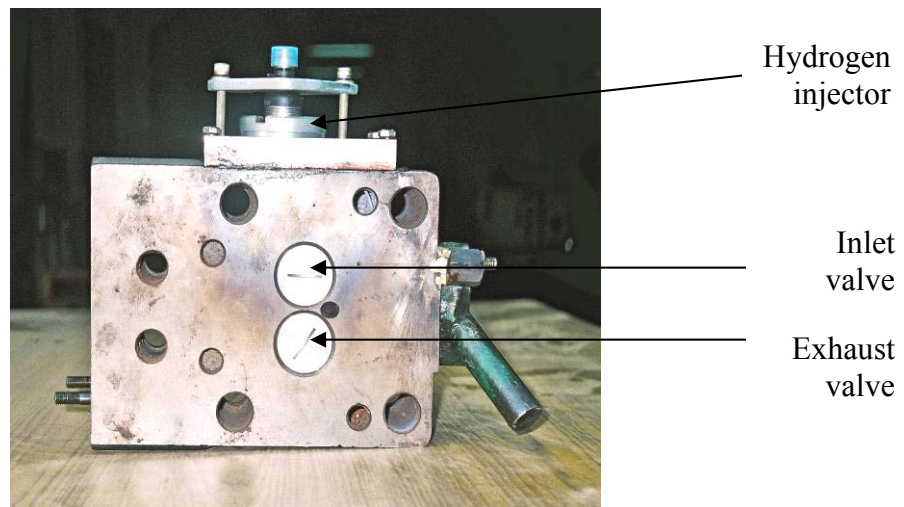


Figure 5. Photographic view of the hydrogen injector position on the cylinder head

4. Instrumentation

The power output of the test engine was measured by an electrical dynamometer. The power capacity of the dynamometer was 10 kW with a current rating of 43.5 amps. The exhaust gas emission was measured by using a Qrotech five gas analyzer. The analyzer was capable of measuring carbon monoxide (CO), carbon dioxide (CO₂) and unburned hydrocarbon (HC) and oxides of nitrogen (NO_x). The analyser uses Non-Dispersive Infra Red (NDIR) principle for the measurement of CO, HC and CO₂. Smoke emissions were measured using a Bosch type smoke meter. The engine cylinder pressure was measured using a water-cooled Kistler piezo electric pressure sensor, which has a sensitivity of 15.2 pC/bar. The charge output of the pressure transducer was amplified by using a kistler charge amplifier. The amplified signals were correlated with the signal from Kistler crank angle encoder having an accuracy of 0.1 degree crank angle and these data were stored on a personal computer for analysis. Table 3 gives the engine specifications. Table 4 gives the instrumentation list. Figure 6 shows the circuit diagram for hydrogen injector. Figure 7 shows the valve timing diagram for hydrogen operation.

Table 2. Properties of hydrogen in comparison with diesel

Properties	Hydrogen (H ₂)	Diesel (C ₁₀ H ₂₂)
Auto Ignition Temperature (K)	858	553
Flammability limits (Volume % in air)	4-75	0.7-5
Molecular Weight (g)	2.016	170
Density of NTP gas (g/cm ³)	0.0838	0.86
Mass Ratio (kg of air/kg of fuel)	34.4	15.2
Flame Velocity (cm/s)	270	30
Specific gravity	0.091	0.83
Heat of Combustion (kJ/kg)	120.0	42.46
Octane Number (R)	130	---
Cetane Number	---	40-60
Boiling Point (K)	20.27	523-630

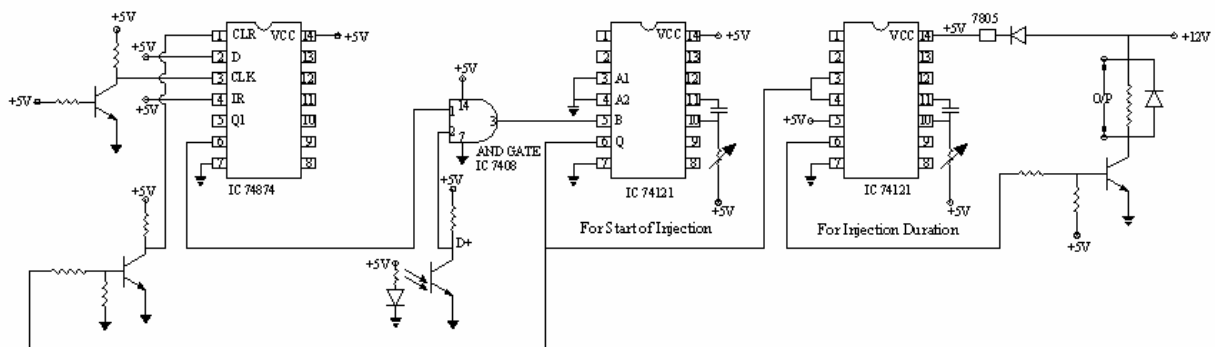


Figure 6. Circuit diagram for hydrogen injector operation

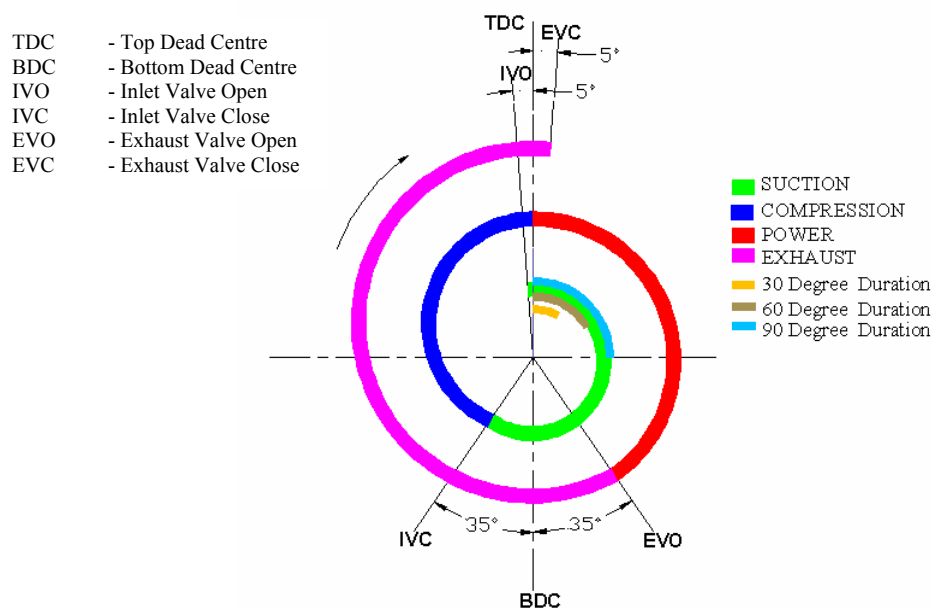


Figure 7. Valve Timing Diagram for hydrogen injection

Table 3. Engine specifications

Make and Model	Kirloskar, AV1 make
General	4-Stroke / Vertical
Type	Compression Ignition
Number of Cylinder	One
Bore	80 mm
Stroke	110 mm
Swept Volume	553 cc
Clearance Volume	36.87 cc
Compression Ratio	16.5: 1
Rated Output	3.7 kW @ 1500 rpm
Rated Speed	1500 rpm
Combustion Chamber	Hemispherical Open
Type of Cooling	Water Cooled

Table 4. Instrumentation list

S.No	Instrument	Purpose	Make / Model
1	Electrical Dynamometer	Measurement of power output	Laurence Scott and elctromotor Ltd., Norwich and Manchester, UK, Capacity-10kW, Current Rating-43 amps.
2	Exhaust Gas Analyser	Measurement of HC, CO, CO ₂ , O ₂ and NOx	QRO 401, Qrotech Corporation Limited, Korea
3	Smoke meter	Measurement of Smoke	TI diesel tune, 114 smoke density tester TI Tran service.
4	Pressure Transducer and Charge Amplifier	Measurement of Cylinder Pressure	Type 5015A, Kistler Instruments, Switzerland.
5	Digital mass flow controller	Measuring the H ₂ flow	DFC 46 mass flow controller AALBORG, USA.
6	Hydrogen Leak Detector	To identify the H ₂ leakage	Finch Mono II, Portable single gas monitor, INIFITRON INC, Korea.

5. Estimation of uncertainty

All measurements of physical quantities are subject to uncertainties. Uncertainty analysis was needed to prove the accuracy of the experiments. In order to have reasonable limits of uncertainty for a computed value an expression was derived as follows:

Let 'R' be the computed result function of the independent measured variables x₁, x₂, x₃,x_n, as per the relation. R = f (x₁, x₂, x_n) and let error limits for the measured variables or parameters be x₁, ± Δx₁, x₂ ± Δx₂, x_a ± Δx_a and the error limits for the computed result be R ± ΔR

To get the realistic error limits for the computed result, the principle of root-mean square method was used to get the magnitude of error given by Holman [19] as;

$$\Delta R = \left[\left(\frac{\partial R}{\partial x_1} \Delta x_1 \right)^2 + \left(\frac{\partial R}{\partial x_2} \Delta x_2 \right)^2 + \dots + \left(\frac{\partial R}{\partial x_n} \Delta x_n \right)^2 \right]^{1/2} \tag{1}$$

Using equation (1) the uncertainty in the computed values such as brake power, brake thermal efficiency and fuel flow measurements were estimated. The measured values such as speed, fuel time, voltage and

current were estimated from their respective uncertainties based on the Gaussian distribution. The uncertainties in the measured parameters, voltage (ΔV) and current (ΔI), estimated by the Gaussian method, are ± 3 V and ± 0.14 A respectively. For fuel time (Δt_f) and fuel volume (Δt), the uncertainties are ± 0.2 sec and ± 0.1 sec respectively. For a Speed (N) of 1500 rpm, Voltage (V) of 230 volts, Current (I) of 14 A, Fuel volume (fx) of 10 cc and brake power (BP) of 3.7 kW the uncertainty in brake power calculation is;

$$BP = \frac{VI}{\eta_g \times 1000} \text{ kW}$$

$$BP = f(V, I)$$

$$\left[\frac{\partial_{BP}}{\partial V} = \frac{I}{(0.86 \times 1000)} = -\frac{14}{(0.86 \times 1000)} = 0.0163 \right]$$

$$\frac{\partial_{BP}}{\partial I} = \frac{V}{(0.86 \times 1000)} = \frac{230}{(0.86 \times 1000)} = 0.2674$$

$$\Delta_{BP} = \left[\sqrt{\left(\frac{\partial_{BP}}{\partial V} \times \Delta V \right)^2 + \left(\frac{\partial_{BP}}{\partial I} \times \Delta I \right)^2} \right]$$

$$= \left[\sqrt{(0.0163 \times 3)^2 + (0.2674 \times 0.14)^2} \right] = 0.185 \text{ kW} \quad (2)$$

Therefore, the uncertainty in the brake power from equation (2) is ± 0.185 kW and the uncertainty limits in the calculation of B.P are 3.6 ± 0.185 kW. Uncertainty in temperature measurement is: $\pm 1\%$ ($T > 150$ °C), $\pm 2\%$ (150 °C $< T < 250$ °C), $\pm 3\%$ ($T < 250$ °C). The uncertainties of other operating parameters are given in Table 5. Appendix 1 shows the mean and standard deviation calculations for 6 samples.

Table 5. Average uncertainties of some measured and calculated parameters

S.No	Parameters	Uncertainty, %
1	Speed	0.6
2	Temperature	0.3
3	Mass flow ratye of air	0.8
4	Mass flow rate of diesel	1.0
5	Mass flow rate of hydrogen	0.2
6	Oxides of nitrogen	0.6
7	Hydrocarbon	0.7
8	Smoke	0.9
9	Particulate matter	1.1

6. Combustion analysis

The details about combustion stages and events can be determined by analyzing the heat release rates as determined from cylinder pressure measurements. Analysis of heat release can help to study the combustion behaviour of the engine.

$$dQ_{hr} = dU + dW + dQ_{ht} \quad (3)$$

Where dQ_{hr} is the instantaneous heat release modeled as heat transfer to the working fluid, dU is the change in internal energy of the working fluid, dW is the work done by the working fluid, and dQ_{ht} is the heat transmitted away from the working fluid (to the combustion chamber walls)

Change in internal energy is given by;

$$dU = C_v/R (PdV + VdP) \quad (4)$$

Work done by the working fluid $dW = pdV$. Heat transfer rate to the wall is given by;

$$dQ_{ht}/dt = h A (T_g - T_w) \quad (5)$$

where R is the gas constant, T , P , V are the temperature, pressure and volume respectively, C_v is the specific heat at constant volume, h is the heat transfer coefficient, and T_w is the temperature of the wall: 400 K.

$$dQ_{ht} = \frac{\gamma}{\gamma-1} p \frac{dV}{d\theta} + V \frac{1}{\gamma-1} \frac{dp}{d\theta} + hA_s (T_g - T_w) \frac{dt}{d\theta} \quad (6)$$

Where θ is the crank angle in degrees. γ is the ratio of specific heats of the fuel and air. A_s is the area in m^2 through which heat transfer from gas to combustion chamber walls take place. The pressure is obtained from the cylinder pressure data at corresponding crank angle.

7. Results and discussions

In exhaust gas recirculation technique, part of the exhaust gases from the engine was cooled down to 30° C and controlled by using a needle valve and admitted along with the intake air in the inlet manifold. Figure 8 and 9 shows the variation of brake thermal efficiency for port and manifold injection for different injection timings. Table 6 gives different injection timings used for hydrogen operation. The optimized conditions in port injection was start of injection at 5° BGTDC, injection duration of 30° CA with hydrogen flow of 7.5 litres/min while the optimized conditions in manifold injection was start of injection at GTDC, injection duration of 30° CA with hydrogen flow of 7.5 litres/min (Table 7). The optimized conditions were chosen based on the improvement in performance and reduction in emissions which was mentioned in detail by the previous work done by the authors [20]. Values of Figure 8 and 9 are given in appendix 2. Table 9 shows the optimized injection timings for hydrogen operation. After optimizing the injection timings the hydrogen flow optimization was done which is depicted in Figure 10 and 11. Since NO_x emission was found to be higher in hydrogen operated engines compared to diesel operation, exhaust gas recirculation technique was adopted for NO_x reduction. The EGR flow rate was varied in steps of 5 % from 5 to 25 % with the above optimized conditions in both port and manifold injection. The engine was operated in the entire load spectrum from no load to full load at different EGR flow rates to study the performance, combustion and emission characteristics of the engine along with the combustion parameters such as peak pressure, heat release rate. Figure 12 and 13 shows the variation of brake thermal efficiency with load for various EGR flows in port and manifold injection. The optimized EGR flow percentage was found to be 20 % in both port and manifold injection. Table 10 shows the various EGR flow percentages used in port and manifold injection.

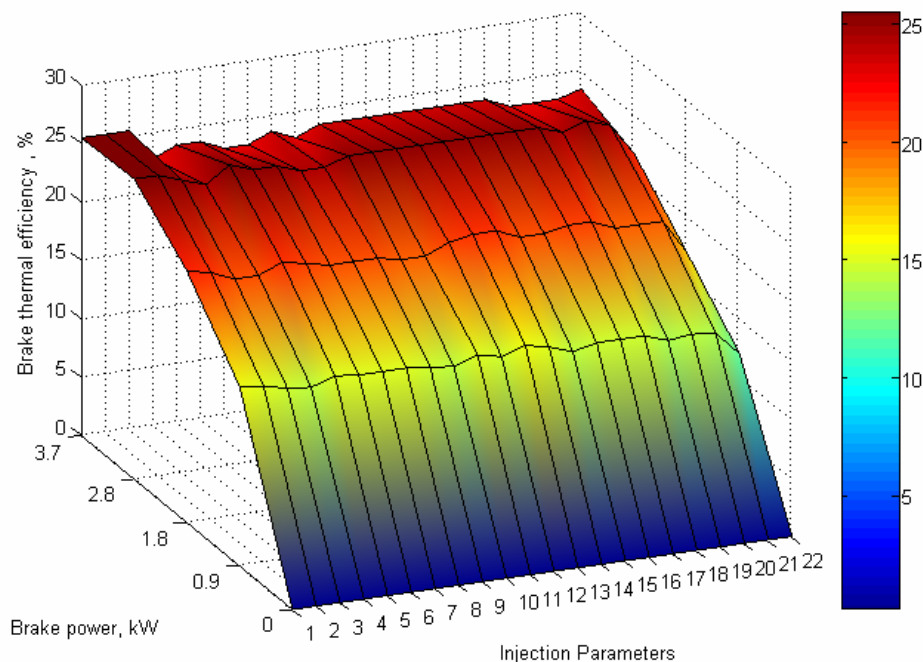


Figure 8. Variation of brake thermal efficiency with brake power for different injection timings and duration (Values are in Table 8) in port injection

Table 6. Start of injection timings and injection duration for hydrogen operation in port and manifold injection

S.No.	Start of Injection		Injection Duration	
	Crank angle (Degrees)	Time (ms)	Crank angle (Degrees)	Time (ms)
1	5° BGTDC	0.555	30	3.33
2	5° BGTDC	0.555	60	6.66
3	5° BGTDC	0.555	90	9.99
4	GTDC	1.110	30	3.33
5	GTDC	1.110	60	6.66
6	GTDC	1.110	90	9.99
7	5° AGTDC	1.665	30	3.33
8	5° AGTDC	1.665	60	6.66
9	5° AGTDC	1.665	90	9.99
10	10° AGTDC	2.220	30	3.33
11	10° AGTDC	2.220	60	6.66
12	10° AGTDC	2.220	90	9.99
13	15° AGTDC	2.775	30	3.33
14	15° AGTDC	2.775	60	6.66
15	15° AGTDC	2.775	90	9.99
16	20° AGTDC	3.330	30	3.33
17	20° AGTDC	3.330	60	6.66
18	20° AGTDC	3.330	90	9.99
19	25° AGTDC	3.885	30	3.33
20	25° AGTDC	3.885	60	6.66
21	25° AGTDC	3.885	90	9.99
22	23° BITDC	Diesel		

Table 7. Optimized injection data for port and manifold injection

Injection Parameter	Port Injection	Manifold Injection
Start of injection of hydrogen	5° BGTDC	GTDC
Hydrogen injection duration	30° crank angle	30° crank angle
Hydrogen flow rate	7.5 litre/min	7.5 litre/min
Exhaust gas Recalculation	20 % EGR	20 % EGR

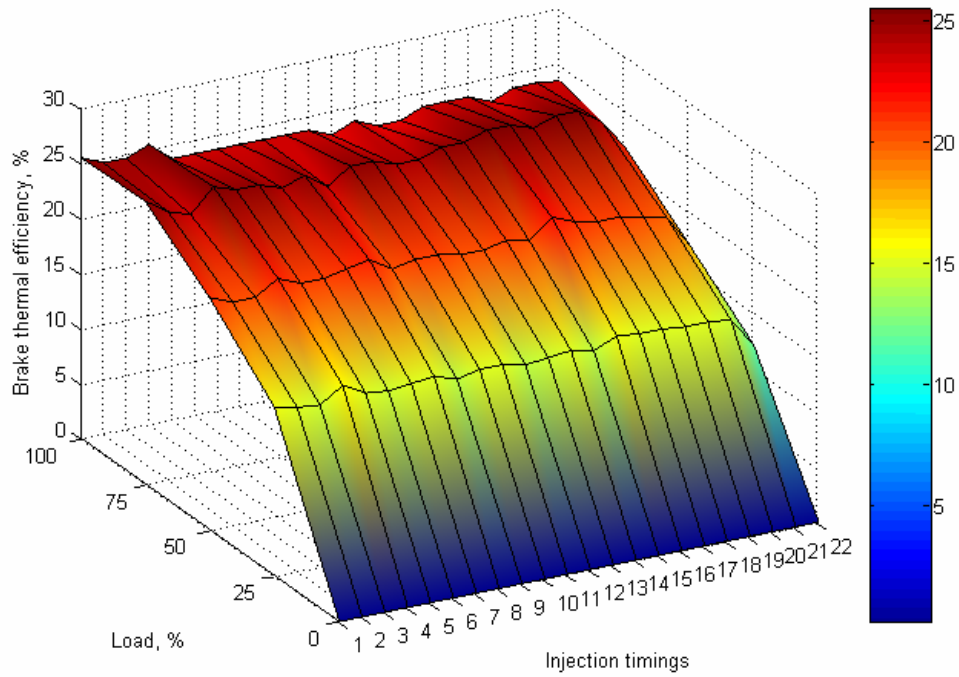


Figure 9. Variation of brake thermal efficiency with brake power for different injection timings and duration (Values are in Table 8) in manifold injection

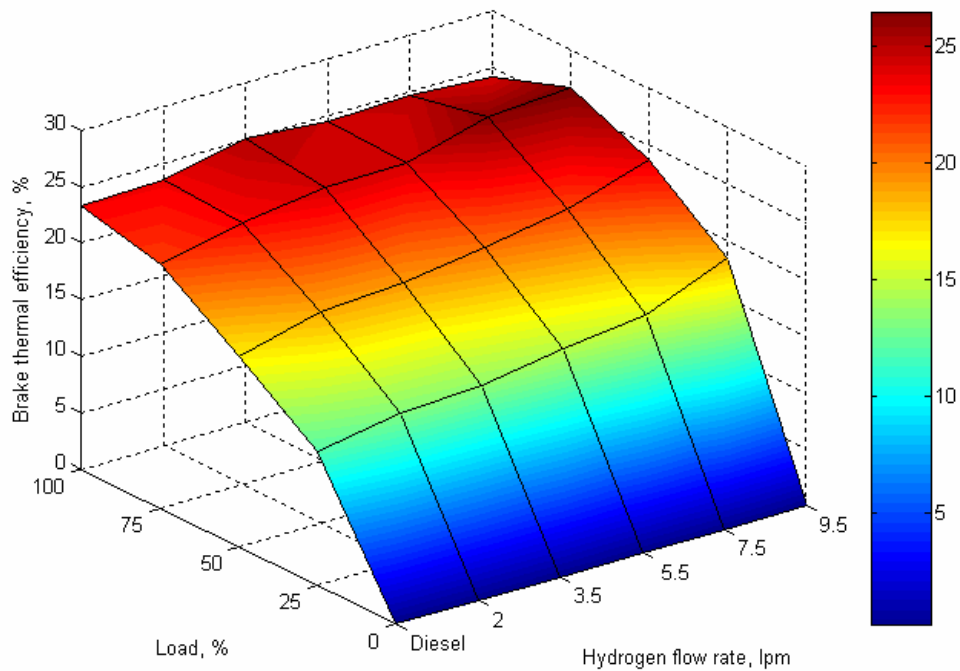


Figure 10. Variation of brake thermal efficiency with load for different hydrogen flow rate in port injection

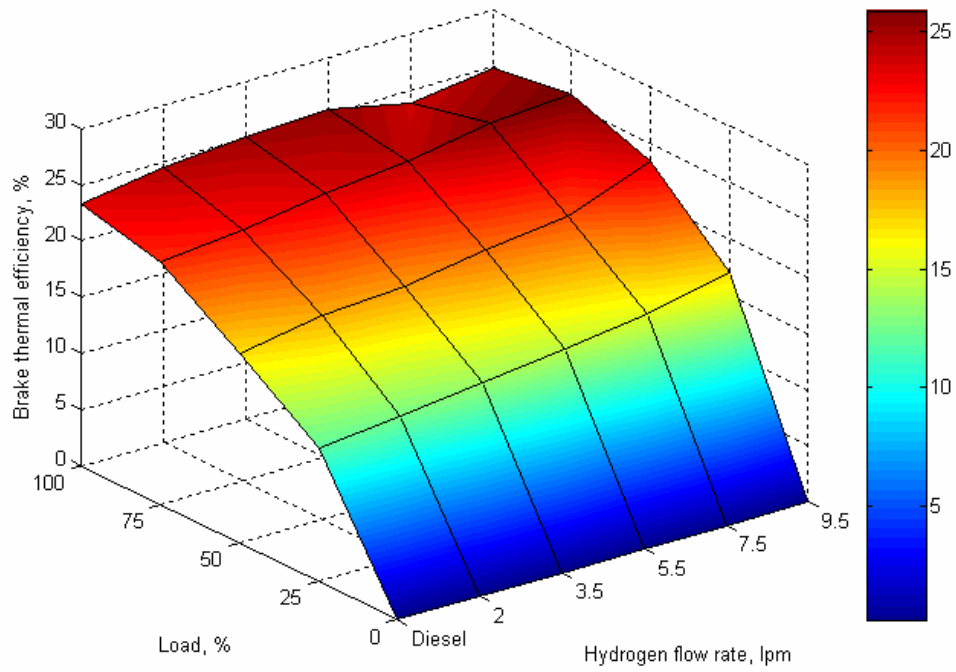


Figure 11. Variation of brake thermal efficiency with load for different hydrogen flow rate in manifold injection

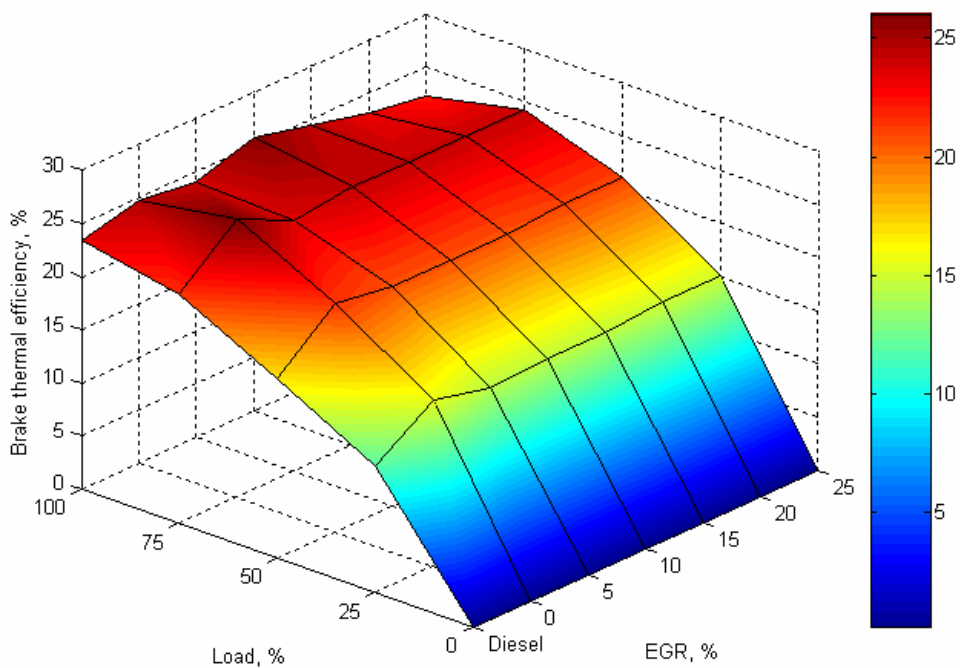


Figure 12. Variation of brake thermal efficiency with load for different EGR flow rate in port injection

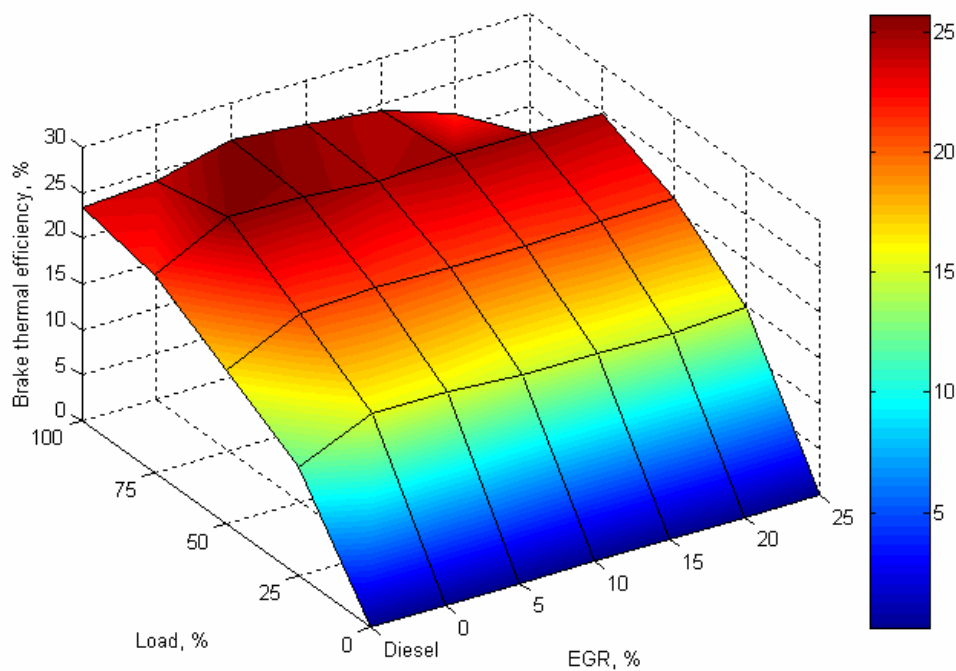


Figure 13. Variation of brake thermal efficiency with load for different EGR flow rate in manifold injection

Table 8. EGR flow percentages used in port and manifold injection

S.No.	Port injection		Manifold injection	
	Optimized timings and duration	EGR flow percentage, (%)	Optimized timing and duration	EGR flow percentage, (%)
1	5° BGTDC, 30° CA, 7.5 litres/min	5	GTDC, 30° CA, 7.5 litres/min	5
2	5° BGTDC, 30° CA, 7.5 litres/min	10	GTDC, 30° CA, 7.5 litres/min	10
3	5° BGTDC, 30° CA, 7.5 litres/min	15	GTDC, 30° CA, 7.5 litres/min	15
4	5° BGTDC, 30° CA, 7.5 litres/min	20	GTDC, 30° CA, 7.5 litres/min	20
5	5° BGTDC, 30° CA, 7.5 litres/min	25	GTDC, 30° CA, 7.5 litres/min	25

7.1 Brake thermal efficiency

Hydrogen combustion exhibits a high cooling loss from the burning gas to the combustion chamber walls compared to hydrocarbon combustion because of its higher burning velocity and shorter quenching distance. These two characteristics have strong influence on the thermal efficiency of hydrogen-operated engines. Indicated thermal efficiency of the engine is given by

$$\eta_i = \eta_{th} \times \eta_{gth} \times \eta_u \times (1 - \phi_w) \quad (7)$$

where η_i is the indicated thermal efficiency, η_{th} is the theoretical thermal efficiency, η_{gth} is the degree of constant volume combustion, η_u is the combustion efficiency, and ϕ_w is the cooling loss ratio

The brake thermal efficiency for hydrogen combustion is

$$\eta_e = \eta_i \times \eta_m \times (1 - \phi_p) \quad (8)$$

where η_e is the brake thermal efficiency, η_m is the mechanical efficiency, and ϕ_p is the pumping loss ratio.

For hydrogen combustion the constant volume degree of combustion (η_{gth}) is 99 % and for diesel it is 90 % whereas $\eta_u \times (1 - \phi_w)$ is 56 % for hydrogen and 61 % for diesel at 10° BITDC. In general by advancing the injection timing η_{gth} increases and $\eta_u \times (1 - \phi_w)$ decreases for both the fuels.

The cooling loss ratio and combustion efficiency are calculated from heat released in a cycle (Q), which is calculated from pressure data, and lower heating value of the fuel supplied (Q_{fuel}).

$$\begin{aligned} \frac{Q}{Q_{fuel}} &= (Q_B - Q_C) / Q_{fuel} \\ \frac{Q}{Q_{fuel}} &= (Q_B - Q_C) \times \eta_u / Q_B \\ \frac{Q}{Q_{fuel}} &= \eta_u \times (1 - \phi_w) \end{aligned} \quad (9)$$

where

$$\phi_w = \frac{Q_C}{Q_B} \quad (10)$$

Q_B is the actual heat release, and Q_C is the cooling loss

Therefore $\frac{Q}{Q_{fuel}}$ corresponds to a function of combustion efficiency η_u and cooling loss ratio ϕ_w . Hence the thermal efficiency of hydrogen combustion engine mainly depends on degree of constant volume combustion and cooling loss to the combustion chamber walls. In order to improve the thermal efficiency of hydrogen operated dual fuel engines the coolant flow was reduced to 75 % of the normal flow and set at 300 lpm for both hydrogen dual fuel operation and diesel to reduce the cooling loss ratio, which causes an increase in thermal efficiency in hydrogen diesel dual fuel operation.

The brake thermal efficiency for hydrogen combustion is

$$\eta_e = \eta_i \times \eta_m \times \eta_{hh} \times (1 - \phi_p) \times 0.99 \times 0.56 = 0.5544 \times \eta_i \times \eta_m \times \eta_{hh} \times (1 - \phi_p) \quad (11)$$

and for diesel is

$$\eta_e = \eta_i \times \eta_m \times \eta_{hh} \times (1 - \phi_p) \times 0.90 \times 0.61 = 0.54 \times \eta_i \times \eta_m \times \eta_{hh} \times (1 - \phi_p) \quad (12)$$

By considering other parameters similar for hydrogen and diesel combustion the brake thermal efficiency in hydrogen combustion is higher compared to diesel combustion. Reducing the cooling loss ratio and operation of engine at leaner equivalence ratios can also increase hydrogen combustion efficiency further.

Brake thermal efficiency is the ratio of brake power to the product of mass flow rate of fuel and calorific value.

$$\eta_e = \frac{bp}{(m_f * cv)_{diesel} + (m_f * cv)_{hydrogen}} \quad (13)$$

$$\eta_e = \frac{3.744}{(1.155 * 43000) + (0.28 * 119930)} = 24.3\% \quad (14)$$

For hydrogen port injection, similarly for diesel it is 21.6 % and for manifold injection it is 25 %. Figure 14 portrays the variation of brake thermal efficiency with load in port and manifold injection. The brake thermal efficiency at 25 % load is found to be 11.9 % in diesel while in port injection with 20 % EGR it is 15 %, in manifold injection it is 14.5 %. The increase in efficiency with EGR at part loads compared to diesel is due to the recirculation of active radicals that enhances the combustion process by providing hotter environment in the combustion chamber. In general the brake thermal efficiency increases with increase in EGR percentage compared to diesel. This is because at no load lean mixture is admitted into the engine cylinder during suction stroke and increasing the quantity of exhaust gases results in the reduction of air-fuel ratio and increases the inlet charge temperature thus enhancing the thermal efficiency of the engine. At 75 % load it can be noticed that the brake thermal efficiency is 24.3 % in port injection with 20 % EGR and 25 % in manifold injection, compared to diesel efficiency of 21.6 %. At full load the brake thermal efficiency decreases with increase in EGR flow rate. It is 23.4 % in diesel while in port injection with 20 % EGR the efficiency is 23.1 % and in manifold injection it is 21.6 %. The reduction in efficiency at full load is due to the high EGR flow rates resulting in deficiency in oxygen concentration in addition to the replacement of air hydrogen. At full load the thermal efficiency in manifold injection drops by 6 % compared to that in port injection with 20 % EGR and the reduction in efficiency is due to smaller replacement of air by hydrogen compared to port injection. The higher specific heat capacity of both CO_2 and H_2O and high flow rates of EGR also reduces the average combustion temperature inside the combustion chamber thus reducing the brake thermal efficiency at full load.

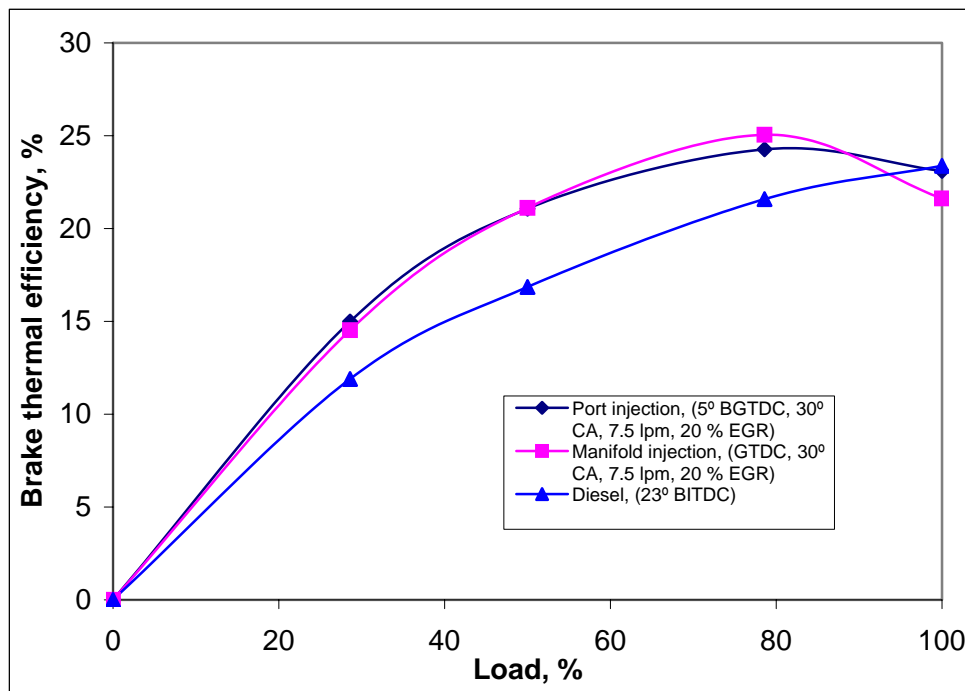


Figure 14. Variation of brake thermal efficiency with load for optimized EGR flow rate of 20 %

7.2 Specific energy consumption

The variation of specific energy consumption with load is depicted in Figure 15 for the optimized flow condition in port injection and manifold injection with 20 % EGR. Specific energy consumption is defined as the amount of energy needed to produce unit kilowatt power. It is observed that the SEC decreases with increase in EGR flow rates at low load conditions. At 25 % load, the SEC with 20 % EGR in port injection is 6.07 and 6.88 in manifold injection compared to diesel of 8.41. At part loads due to the recycling of exhaust gases the inlet charge temperature increases which leads to accelerated combustion resulting in the reduction of SEC compared to diesel. The SEC in port injection is 4.12 while in manifold injection it is 3.99 and for diesel it is 4.63 at 75 % load. At full load, the SEC increases with EGR flow rates. In port injection the SEC is 4.33 and in manifold injection it is 4.62 compared to 4.28 in diesel. The SEC in port injection is lesser compared to that in manifold injection. At 75 % load, with 20 % EGR the SEC reduces by 3 % in port injection at full load compared to 7 % in manifold injection. With increase in EGR flow percentages at part loads the SEC drops due to the replacement of air by inert

gases which improve the over all charge temperature at part loads resulting in SEC reduction. At full load less air is admitted due to replacement of air by hydrogen and EGR. Hence more fuel is admitted to attain the rated power, which results in an increase in SEC. Table 9 gives the energy share ratio of hydrogen to diesel in port injection. Table 10 gives the energy share ratio of hydrogen to diesel in manifold injection.

Table 9. Energy share ratio of hydrogen to diesel for optimized port injection (5° BGTDC, 30° CA, 7.5 litres/min, 20 % EGR)

Load, %	Hydrogen energy, %	Diesel energy, %
No load	33.01	66.99
25 % load	21.54	78.46
50 % load	16.58	83.42
75 % load	11.64	88.36
Full load	09.17	90.83

Table 10. Energy share ratio of hydrogen to diesel for optimized manifold injection (5° AGTDC, 30° CA, 7.5 litres/min, 20 % EGR)

Load, %	Hydrogen energy, %	Diesel energy, %
No load	33.75	66.25
25 % load	20.74	79.26
50 % load	16.63	83.37
75 % load	12.07	87.93
Full load	08.54	91.46

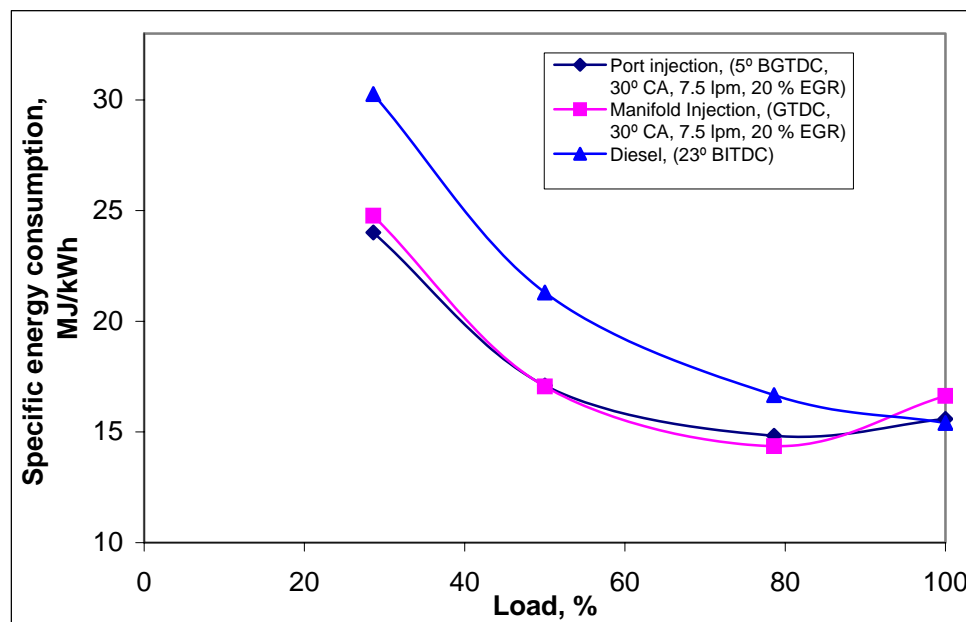


Figure 15. Variation of specific energy consumption with load for optimized EGR flow rate of 20 %

7.3 Oxides of nitrogen

Nitric oxide (NO) and nitrogen dioxide (NO₂) are usually grouped together as NO_x emissions. NO₂/NO in a diesel engine is approximately in the ratio of 10 to 30 percent. The mechanism of NO formation given by Zeldovich is:



The NO formation rate is derived from the equation

$$\frac{d[\text{NO}]}{dt} = \frac{6 \times 10^{16}}{T^{1/2}} \exp\left(\frac{-69090}{T}\right) [\text{O}_2]_e^{1/2} [\text{N}_2]_e \quad (18)$$

where $\frac{d[\text{NO}]}{dt}$ is NO formation rate, T is the temperature, O_2 is the oxygen concentration at equilibrium condition, and N_2 is the nitrogen concentration at equilibrium condition

In port injection, manifold injection and diesel the peak pressure is 67, 65.5, 63.4 bar respectively at 25 % load. The initial temperature and pressure is 303 K and 1 bar respectively. The peak combustion temperature for diesel is calculated from peak pressure by using the equation.

$$\frac{T_2}{T_1} = (r)^{(\gamma-1)} \quad (19)$$

where r is the compression ratio of the engine which is 16.5 and γ is specific heat ratio which is 1.4 for hydrogen and air.

$$T_2 = (16.5)^{0.4} \times 303$$

$$T_2 = 929.9 \text{ K}$$

$$\frac{p_2}{p_1} = (r)^\gamma \quad (20)$$

$$p_2 = (16.5)^{1.4} = 50.63 \text{ bar}$$

$$\frac{T_3}{T_2} = \frac{p_3}{p_2} \quad (21)$$

$$T_3 = (67/50.63) \times 929.89$$

$T_3 = 1230 \text{ K}$ for diesel, similarly for port injection it is 1202 K and for manifold injection it is 1164 K. The corresponding NO_x values are 25.6, 22.04, 18.5 g/kWh. From the values it can be found that NO_x is mainly dependent on temperature.

The time calculation for NO is

$$\tau_{NO} = \frac{8 \times 10^{-16} T \exp(58300 / T)}{p^{1/2}} \quad (22)$$

where τ_{NO} is in seconds

NO concentration is found to be 5×10^{-8} moles/cm³ at time 5 ms and 10^{-7} at characteristics time of 10 ms at an equivalence ratio of 1 for hydrogen air mixtures. As the residence time increases the NO_x formation will also increase. It can be observed that temperature is the main factor for the formation of NO compared to the availability of oxygen. In diesel engines the combustion is always leaner that results in the availability of more oxygen for the entire load spectrum of operation. NO formation in a diesel combustion peaks at critical time period (between start of combustion and shortly after the occurrence of peak cylinder pressure).

The variation of NO_x with load is depicted in Figure 16 for optimized port and manifold injection system with EGR. Generally the NO_x emission tends to reduce significantly with increase in EGR percentages at all the load conditions due to the rise in total heat capacity of the working gases, which lowers the elevated temperature [21]. At 25 % load the NO_x is observed to be of 8.32 g/kWh with 20 % EGR in port injection with an optimized timing of 5° AGTDC, duration of 30° CA and hydrogen flow rate of 7.5 litres/min, while in manifold injection it is observed to be 8.78 g/kWh with an optimized injection timing of GTDC, injection duration of 30° CA and optimum hydrogen flow of 7.5 litres/min. While for 20 % EGR in port injection the NO_x is observed to be 7.35 g/kWh in manifold injection it is 6.55 g/kWh compared to diesel of 18.11 g/kWh. At full load the NO_x emission decreases from 16.13 g/kWh in diesel

to 3.78 g/kWh with 20 % EGR in port injection and further to 2.43 g/kWh in manifold injection. The NO_x emission reduces with increase in EGR flow percentage, due to the presence of inert gas (CO_2 and H_2O) inside the combustion chamber, which reduces the peak combustion temperature, in addition to the replacement of oxygen. As a result of reduction in both the parameters the NO_x percentage reduces with the use of EGR. Compared to that of port injection, manifold injection shows a reduction in NO_x by 11 % at 75 % load and 35 % at full load with 20 % EGR. NO_x reduces by 4 fold in port injection and 6 fold in manifold injection with EGR at full load compared to diesel. After the occurrence of peak pressure the burned gas temperature decreases as the cylinder gets expanded which makes the combustion temperature to decrease resulting in freezing of NO. In hydrogen diesel combustion the rate of pressure rise is maximum in port injection, 7.1 bar/ $^\circ\text{CA}$ at 355 $^\circ$ CA followed by 7 bar/ $^\circ\text{CA}$ at 356 $^\circ$ CA in manifold injection and, 6.63 bar/ $^\circ\text{CA}$ in diesel at 356 $^\circ$ CA at full load (Figure 23). The ignition delay or delay period is found to be 11 $^\circ$ or 1.22 ms in diesel and in port injection it is 9 $^\circ$ or 1 ms and in manifold injection it is 10 $^\circ$ or 1.11 ms that makes the combustion to be rapid and ends instantaneously resulting in increase in NO. The hydrogen combustion duration is shorter due to its high burning velocity (2.65-3.25 m/s for hydrogen and 0.3 m/s for diesel) compared to diesel. In general the NO formed in hydrogen-diesel dual fuel operation is higher for both port and manifold injection compared to diesel operation.

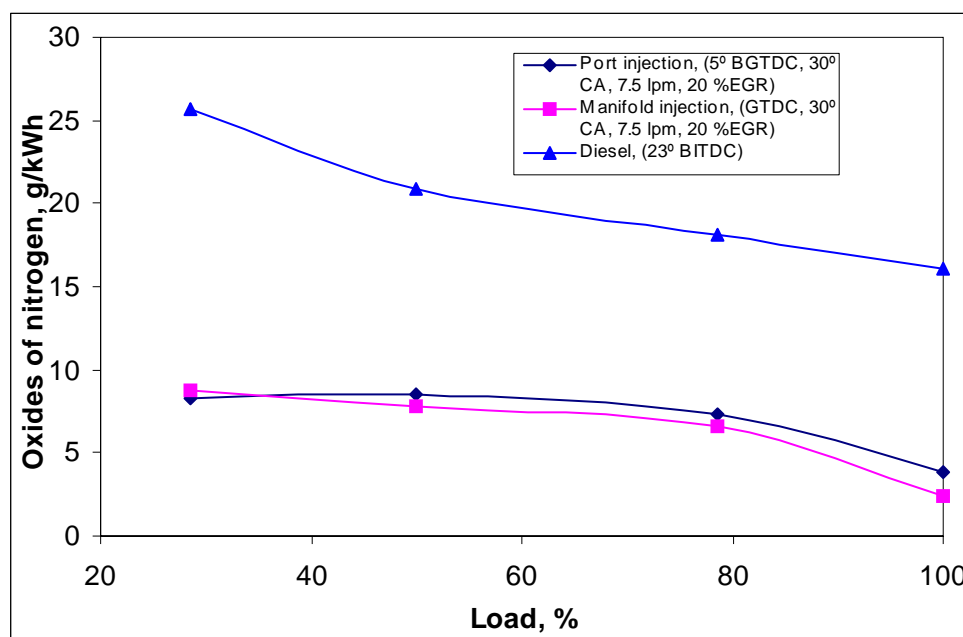


Figure 16. Variation of oxides of nitrogen with load for optimized EGR flow rate of 20 %

7.4 Smoke

Diesel particulate or smoke consist principally combustion generated carbonaceous materials (soot) on which some organic compounds have been absorbed. Most particulate material results from incomplete combustion of fuel hydrocarbons and the lubricating oil contributes some. The equation for the formation of smoke is



If $m > 2y$, then C/O ratio exceeds unity resulting in the formation of smoke. The fuel air ratio for smoke formation is given by

$$\phi = 2 \left(\frac{C}{O} \right) (1 + \delta) \quad (24)$$

Where $\delta = n / 4m$, ϕ is 3 for $(C/O) = 1$ with $n/m = 2$. Since carbon is not present in hydrogen smoke will not be formed. In hydrogen diesel dual fuel operated engine due to the presence of hydrogen the net smoke emission decreases. Figure 17 shows the variation of smoke with load for different EGR flow percentage for port and manifold injection. The smoke emission reduces with both increase in hydrogen and with increase in EGR percentage. Even with EGR, the smoke concentration is lesser than diesel upto

75 % load but it increases in full load condition due to richening of gas-air mixture, promoting the combustion [22]. Smoke of 0.3 BSN is observed with diesel at no load condition while in port injection with 20 % EGR it is 0.1 BSN and no smoke is observed in manifold injection. At 75 % load in diesel 2.2 BSN is observed while in port injection with 20 % EGR the smoke is 1.9 BSN and in manifold injection it is 2.2 BSN. Similarly at full load smoke of 3.6 BSN is observed for diesel, 4.9 BSN with 20 % EGR in port injection and 5.2 BSN in manifold injection. Compared to port injection, manifold injection emits smoke about 5 % higher at 75 % load and full load. At higher loads with high EGR flow rates, the intensity of smoke is higher which may be due to the reason that, some of the oxygen in the inlet charge is replaced by recycled exhaust gases results in improper combustion.

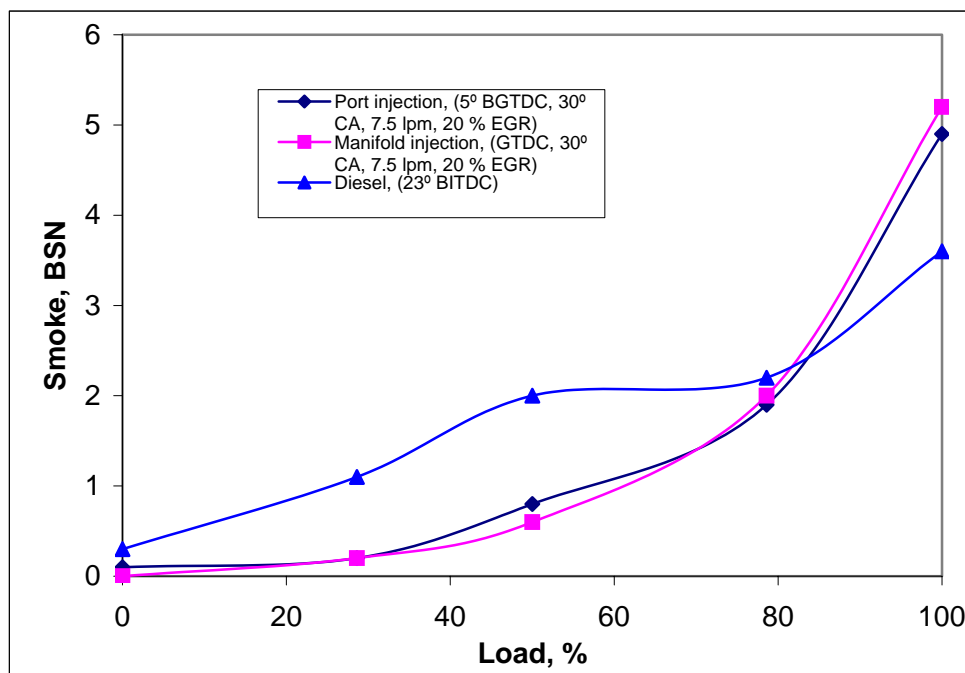


Figure 17. Variation of smoke with load for optimized EGR flow rate of 20 %

7.5 Carbon monoxide

The CO formation in the hydrocarbon radical is given by the reaction



R stands for the hydrocarbon radical. CO formed through the combustion process will then be oxidized to CO₂ at a slower rate. The CO oxidation reaction in hydrocarbon-air flame is given by the equation



Based on the oxygen availability the CO formed during the combustion is oxidized further to form CO₂. In general in hydrogen diesel dual fuel operation at full load condition combustion takes place in a slightly richer mixture than normal diesel combustion due to the air replacement by hydrogen in the intake manifold that causes a marginal increase in CO concentration. The variation of CO with load is shown in Figure 18 for port and manifold injection with EGR flow rate of 20 %. The CO emission at no load and full load is higher in manifold injection. An increase in EGR percentage at no load does not show a dramatic effect on CO variation. At 25 % load the CO concentration is found to be 0.65 g/kWh in diesel while in port injection with 20 % EGR it is 0.43 g/kWh and in manifold injection it is 1.29 g/kWh. The reduction in CO at 25 % load is due to the use of EGR creating a hotter environment, which makes an improvement in combustion in comparison with diesel in port injection. At 75 % load the CO emission is found to be 0.63 g/kWh in port injection with 20 % EGR and 0.55 g/kWh in manifold injection compared to diesel of 0.32 g/kWh. At full load with increase in EGR percentage the CO concentration increases. At full load the CO concentration in diesel is 0.88 g/kWh while for 20 % EGR in port injection it is 4.65 g/kWh and in manifold injection it is 9.33 g/kWh. The increase in CO concentration is due to the partial replacement of oxygen in inlet air by inert gases, which results in deficit in oxygen concentration.

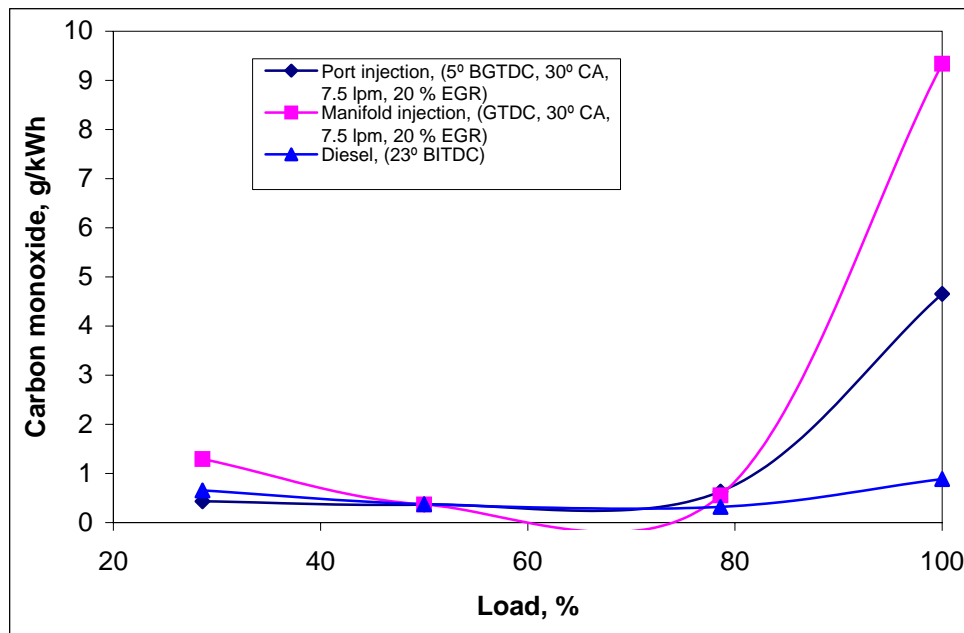


Figure 18. Variation of carbon monoxide with load for optimized EGR flow rate of 20 %

7.6 Carbondioxide

Figure 19 depicts the variation of CO₂ with load for port injection and manifold injection system with 20 % EGR flow rate. Carbon dioxide is a principal constituent of exhaust gases. The nature of CO₂ is higher heat capacity and it serves as a heat absorbing agent during combustion, which reduces the peak temperature in the combustion chamber. The CO₂ concentration decreases in general for various EGR percentages. At no load the concentration of CO₂ in diesel is found to be 1.30 g/kWh compared to 0.97 g/kWh in port injection and 0.99 g/kWh in manifold injection at 25 % load. The reduction in CO₂ concentration is due to the replacement of diesel with hydrogen induction with air. At 75 % load the lowest CO₂ of 0.68 g/kWh can be observed in port and manifold injection with 20 % EGR compared to diesel of 0.78 g/kWh. At full load the CO₂ concentration is found to be 0.50 g/kWh in manifold injection and 0.57 g/kWh in port injection compared to diesel of 0.76 g/kWh. At full load not only the concentration of hydrogen reduces the CO₂ concentration, but also instability in combustion and deficiency of oxygen makes the CO concentration to increase and CO₂ concentration to decrease at high load.

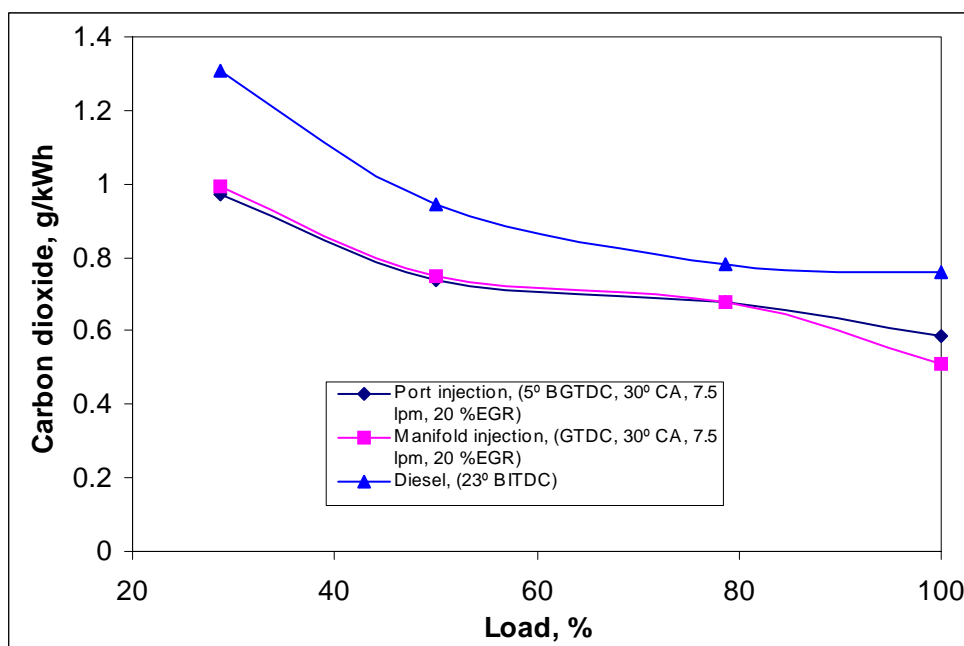


Figure 19. Variation of carbon dioxide with load for optimized EGR flow rate of 20 %

7.7 Hydrocarbon

Hydrocarbons are organic emissions that result as a consequence of incomplete combustion of fuel. Hydrocarbon oxidation rate is:

$$\frac{d[HC]}{dt} = -6.7 \times 10^{15} \exp\left(\frac{-18735}{T}\right) x_{HC} x_{O_2} \left(\frac{p}{RT}\right) \quad (27)$$

where x_{HC} and x_{O_2} are the mole fraction of HC and O_2 , dt is the difference in time in seconds, and T is the temperature in kelvins.

The reason for the increase in HC emission is due to extremely lean mixture (mixture becomes too lean to auto ignite) and the longer ignition delay period. A small increase in ignition delay by 2° CA causes an increase in HC emission by 60-70 %. For hydrogen diesel dual fuel operation the delay period is lower, due to the rapid combustion of hydrogen that assists diesel combustion resulting in a reduction in delay period. The ignition delay or delay period is found to be 11° or 1.22 ms in diesel, 9° or 1 ms in port injection and 10° or 1.1 ms in manifold injection.

The variation of HC with load is shown in Figure 20 in port and manifold injection using EGR. At 25 % load HC of 0.27 g/kWh can be observed for diesel and 0.28 g/kWh in port injection and 0.11 g/kWh in manifold injection. The decrease in HC in manifold injection compared to port injection is due to more time available for mixing hydrogen with air. At 75 % load the HC is found to be 0.14 g/kWh in port injection and 0.13 g/kWh in manifold injection compared to diesel of 0.13 g/kWh. At full load the HC is observed to be 0.20 g/kWh in manifold injection and 0.16 g/kWh in port injection compared to diesel of 0.13 g/kWh. The increase in HC is due to the flame quenching at part load condition and reduction in oxygen in the inlet charge by the EGR admitted into the cylinder [23]. Compared to port injection an increase in HC in the order of 25 % is noticed in manifold injection at full load with 20 % EGR. The increase may be due to the large replacement of oxygen in the inlet charge.

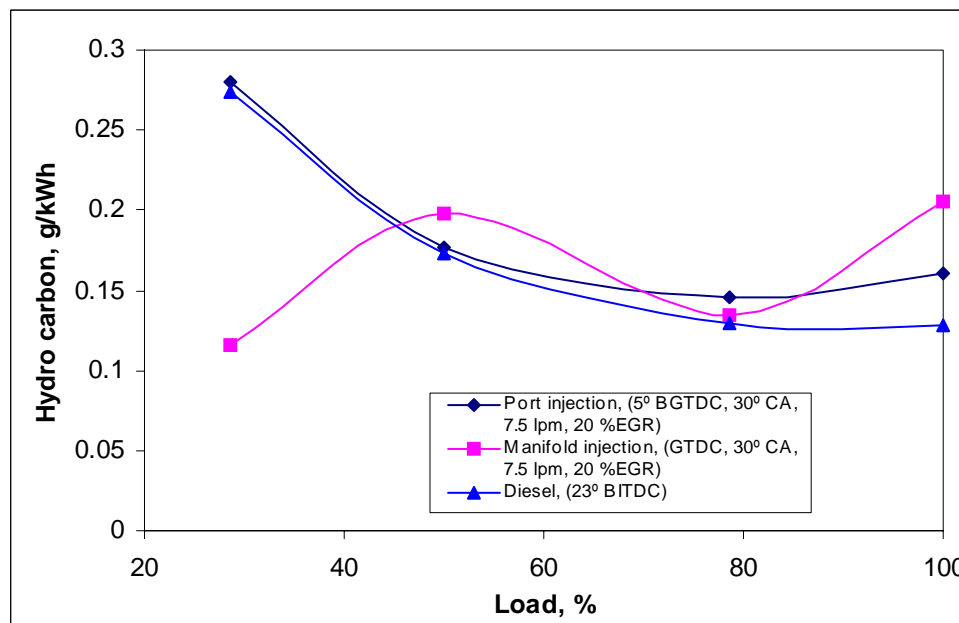


Figure 20. Variation of hydrocarbon with load for optimized EGR flow rate of 20 %

7.8 Variation of peak pressure

The ignition delay depends on the physical and chemical process. The physical process includes the atomization of liquid fuel, the vaporization of the fuel droplet, mixing of fuel vapor with air. The chemical processes are the pre-combustion reactions of the fuel and air, residual gas mixture (which leads to auto ignition). The delay processes are affected by engine design and operating variables in addition to the fuel characteristics.

By using hydrogen in the dual fuel mode in diesel engine it reduces the chemical delay period resulting in the reduction of ignition delay period. In diesel engines ignition occurs in vapor phase and oxidation reactions proceed in the liquid phase as well as between the fuel molecules. The oxygen dissolved in fuel droplets also cracks large hydrocarbon molecules into smaller molecules. These chemical processes

depend on the composition of the fuel, the cylinder charge temperature and pressure as well as the physical process. In hydrogen diesel dual fuel combustion process as soon as the ignition is initiated by diesel combustion hydrogen also undergoes simultaneous and spontaneous combustion. As hydrogen is already mixed uniformly with air makes the combustion to be faster. Further it also assists diesel combustion by breaking the larger hydrocarbons of diesel fuel and makes the diesel combustion also faster. Hence the delay period for the hydrogen diesel dual fuel combustion is reduced.

The ignition delay for the diesel combustion is calculated by the equation

$$\tau_{id}(CA) = (0.36 + 0.22S_p) \exp \left[E_A \left(\frac{1}{RT} - \frac{1}{17190} \right) \left(\frac{21.2}{p-12.4} \right)^{0.63} \right] \quad (28)$$

where τ_{id} is the ignition delay in crank angles, T is the temperature in kelvins, p is the pressure in bars

S_p is the mean piston speed in metre per second, R is the universal gas constant (8.3143 J/mol K), and

E_A is the apparent activation energy in joules per mole.

$$E_A = \frac{618840}{CN + 25} \quad (29)$$

where CN is the cetane number of the fuel used. The apparent activation energy decreases with increase in cetane number.

Ignition delay in milliseconds is given by

$$\tau_{id}(ms) = \frac{\tau_{id}(CA)}{0.006N} \quad (30)$$

where N is the engine speed in rpm

The temperature and pressure can be calculated from the combustion data.

$$T_{TC} = T_i r_c^{n-1} \quad (31)$$

$$p_{TC} = p_i r_c^n \quad (32)$$

where TC is the compression air temperature, n is the polytropic exponent, r_c is the compression ratio, and i denotes the intake condition

From the above equations it is observed that pressure and temperature are the main factors for ignition delay. As the pressure and temperature increases the ignition delay gets reduced. In hydrogen diesel dual fuel combustion the rate of pressure rise and the temperature inside the combustion chamber is higher which results in the reduction of delay period. The rate of pressure rise in hydrogen diesel dual fuel operation in port injection is 7.1 bar/°CA while it is 6.63 bar/°CA for diesel at full load. The ignition delay is found to be 9° or 1 ms for hydrogen diesel dual fuel operation compared to 11° or 1.22 ms in diesel. The peak pressure for hydrogen diesel dual fuel operation in port injection is higher by 2-3 bar compared to diesel at full load.

Figure 21 depicts the variation of peak pressure with load. In general an increase in EGR flow rate may result in peak cylinder pressure to decrease. At 75 % load it is found that the lowest peak pressure of 73 bar is observed with 20 % EGR in port injection compared to 73.1 bar in manifold injection and 78.5 bar in diesel. At full load the peak pressure is 76.6 bar in port injection and in manifold injection it is 76.1 bar compared to diesel peak pressure of 82.2 bar. The reduction in peak pressure is due to the replacement of air by inert gas CO₂ and other constituent such as water, which acts as diluents and heat sink that results in peak pressure reduction. Compared to port injection, manifold injection gives lesser peak pressure. With 20 % EGR at 50 % load, port injection shows higher peak pressure of 3 % compared to manifold injection. Similarly at full load with 20 % EGR, the peak pressure in port injection increases by 1 % compared to manifold injection. The increase in peak pressure in port injection is due to the rapid combustion that takes place in the combustion chamber as the time available for mixing the hydrogen and air is lesser compared to manifold injection. The use of EGR also reduces the peak pressure, which eliminates the knocking problem during high hydrogen flow rates at full load.

7.9 Pressure crank angle diagram

Figure 22 shows the pressure crank angle diagram for optimized EGR of 20 % in port injected hydrogen and manifold injected hydrogen and diesel at 75 % load. The peak pressure in diesel is 78.5 bar and 70.08 bar with 20 % EGR in port injection and 73.5 bar in manifold injection. The peak pressure reduces by 5 % in port injection compared to manifold injection and there is a shift in peak pressure towards TDC by 2° compared to that of hydrogen injection. The shift is due to the increase in delay period due to the presence of exhaust gases.

7.10 Heat release rate

Figure 23 depicts the heat release rate for port-injected hydrogen, manifold injected hydrogen with 20 % EGR and diesel at 75 % load. A reduction in peak heat release rate in EGR operation is observed. The peak heat release decreases from 55.3 J /° CA in diesel to 47.89 J /° CA with 20 % EGR in port injection and to 53.49 J /° CA in manifold injection. A progressive shift in heat release pattern with increase in EGR percentage can be noticed, which is due to the reduction in oxygen concentration and by the addition of CO₂. The increase in ignition delay provides more time for the fuel to mix with oxygen and a reduction in oxygen concentration reduces the intensity of peak heat release. The use of diluents CO₂ and H₂O, which are the principal constituents of EGR, results in an increase in ignition delay and a shift in the start of combustion towards ITDC. The shift in the start of combustion towards expansion stroke results in shorter combustion duration which can also be seen from the rate of pressure rise.

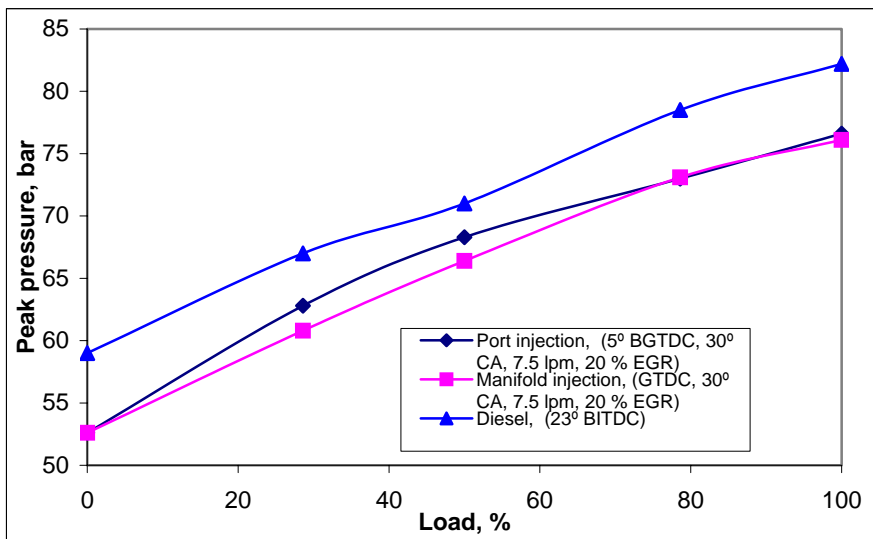


Figure 21. Variation of peak pressure with load for optimized EGR flow rate of 20 %

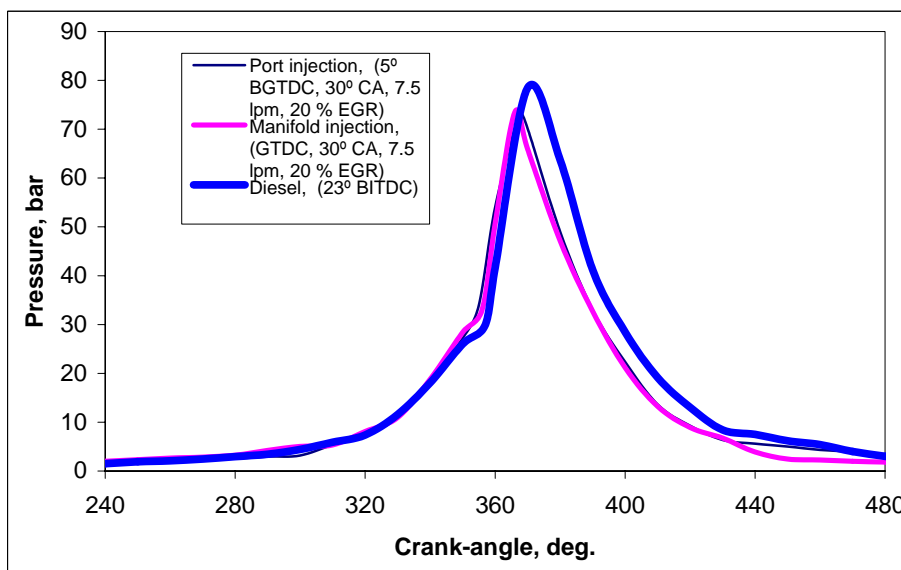


Figure 22. Pressure crank angle at 75 % load for optimized EGR flow rate of 20 %

7.11 Rate of pressure rise

Figure 24 depicts the variation rate of pressure rise with crank angle for port and manifold injection at 75 % load 20 % EGR. The start of injection in diesel is at 23° BITDC. The ignition delay or delay period is found to be 11° or 1.22 ms in diesel and in port and manifold injection it is 12° or 11.33 ms respectively. As the combustion starts the rate of pressure rise increases in a progressive manner compared to diesel in hydrogen due to the presence of exhaust gases [24]. The rate of pressure rise is maximum in manifold injection, 4.43 bar/°CA at 356° CA followed by 4.01 bar/°CA at 355° CA in port injection and 3.9 bar/°CA for diesel at 357° CA at 75 % load. The increase in rate of pressure rise is due to the instantaneous combustion taking place due to hydrogen. The rate of pressure rise is higher by about 10 % in the case of manifold injection compared to port injection due to the uniform mixture formation in manifold injection. The combustion duration in port injection is 21° CA and in manifold injection it is 18° CA compared to diesel of 26° CA. The extended combustion in port injection is due to non-uniformity in fuel mixture making the combustion to extend by about 3° CA compared to manifold injection.

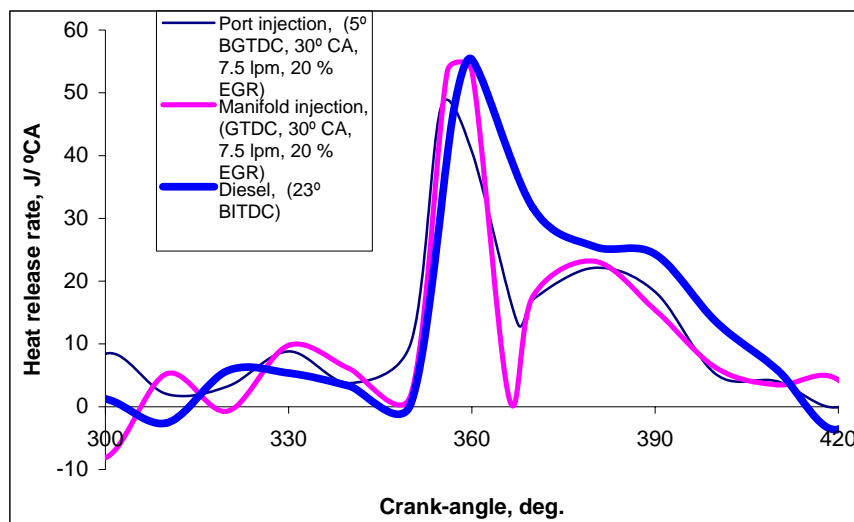


Figure 23. Heat release rate at 75 % load for optimized EGR flow rate of 20 %

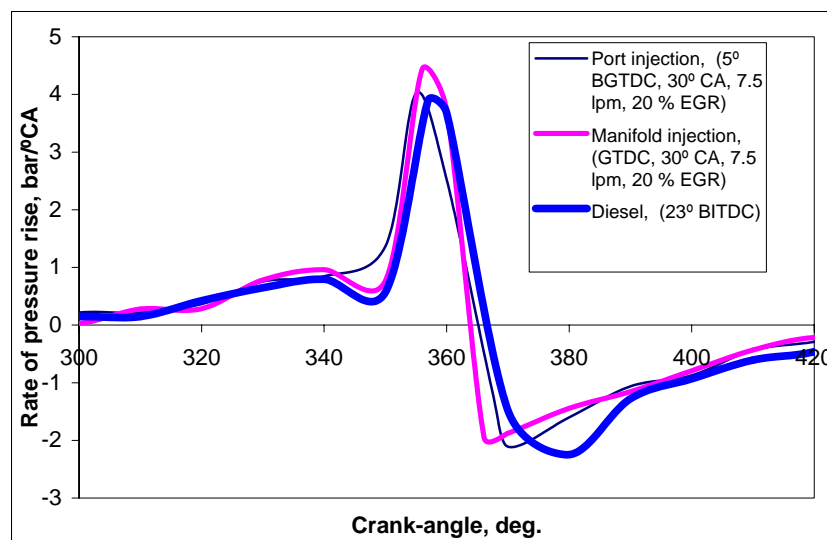


Figure 24. Rate of pressure rise with crank angle at 75 % load for optimized EGR flow rate of 20 %

8. Conclusion

Experiment has been conducted on a single cylinder diesel engine to operate under hydrogen diesel dual fuel mode. From the results it was observed that in manifold injection technique the optimized condition is start of injection at GTDC with injection duration of 30° crank angle with the hydrogen flow rate of 7.5 litres/min with 20 % EGR. In port injection technique, the optimized condition is start of injection at 5°

BGTDC with injection duration of 30° CA with the hydrogen flow rate of 7.5 litres/min with 20 % EGR. Brake thermal efficiency in port injection increases by 13 % and 16 % in manifold injection at 75 % load with 20 % EGR. As for the NO_x and smoke tradeoff is considered with EGR there is a greater reduction in both NO_x emission and smoke the NO_x reduces by almost 3 times in both port injection and manifold injection and smoke emission reduces by 13 % in port injection and 9 % in manifold injection. Since the diesel engine is mainly operated at part load of 75 % this reduction in emissions will result in significant drop in emissions. However at full load the NO_x reduction is still higher by 4 times in port injection and 7 times in manifold injection however there is an increase in smoke by 36 % in port injection and 44 % in manifold injection. The CO emission is found to be increases however CO₂ emission decreases making the overall carbon emission to reduce compared to diesel. There is slight increase in HC emission is also observed. In general with the use of EGR the emissions are found to be decreased with a significant improvement in performance with hydrogen and EGR.

Appendix 1

Example for Diesel fuel and Hydrogen port injection												
	Trial-1(x1)	Trial-2(x2)	Trial-3(x3)	Trial-4(x4)	Trial-5(x5)	Trial-6(x6)	Avg. (x)	SD	Deviati on	Value should lie between		
Load, %	EG1	2	3	4	5	6	EG(mea n)		(1.96*S D)	Average EG (+ or -)1.96SD		
Diesel												
No load	197	190	192	192	190	194	192.500	2.665	5.223	197.723	to	187.277
28.6	254	251	249	247	252	260	252.167	4.140	8.114	260.281	to	244.052
50.0	322	312	323	315	329	318	319.833	6.113	11.981	331.814	to	307.852
78.6	378	381	385	393	383	394	385.667	5.935	11.632	397.299	to	374.034
100.00	452	449	461	465	456	463	457.667	6.377	12.499	470.166	to	445.168
Hydrogen port Injection												
No load	195	199	191	190	200	195	195.000	4.050	to	202.937	to	187.063
28.6	258	259	253	249	262	255	256.000	4.243	8.316	264.316	to	247.684
50.0	308	314	305	297	306	314	307.333	6.377	12.499	319.832	to	294.834
78.6	392	400	397	380	393	400	393.667	6.848	13.421	407.088	to	380.245
100.0	489	476	481	480	474	489	481.500	6.348	12.443	493.943	to	469.057

Appendix 2

Brake Thermal Efficiency for port injection for different injection timings (Figure 8)																						
Load %	1	2	3	4	5	6	7	8	9	10	11	12	13	14	15	16	17	18	19	20	21	22
28.6	15.3	15.1	14.6	14.4	15.1	14.8	14.8	14.8	14.6	14.4	15.1	14.6	15.3	14.8	14.2	14.6	14.6	14.6	13.9	14.2	13.9	11.9
50.0	21.5	21.1	20.2	20.2	21.1	20.6	20.2	20.2	20.2	19.8	19.8	20.6	21.1	21.1	20.2	20.2	20.6	20.6	19.8	19.8	19.8	16.9
78.6	25.7	25.7	25.0	24.3	25.7	25.0	25.0	24.3	24.3	25.0	25.0	25.0	25.0	25.0	25.0	25.0	25.0	25.0	24.3	25.0	24.3	21.6
100.0	25.5	25.5	25.5	22.8	23.6	23.6	22.8	22.8	23.6	22.8	23.6	23.6	23.6	23.6	23.6	23.6	23.6	23.6	22.8	22.8	22.8	23.4
Brake Thermal Efficiency for manifold injection for different injection timings (Figure 9)																						
Load %	1	2	3	4	5	6	7	8	9	10	11	12	13	14	15	16	17	18	19	20	21	22
28.6	15.3	14.8	14.6	16.0	14.8	14.6	14.8	15.1	14.4	14.8	14.8	14.4	14.6	14.8	14.4	15.3	15.1	15.1	14.8	14.8	14.6	11.9
50.0	21.1	20.2	20.2	21.5	20.6	20.6	21.1	21.5	20.2	20.6	20.6	20.2	20.2	20.6	20.2	21.9	21.1	20.6	20.6	20.2	19.8	16.9
78.6	25.7	24.3	23.6	25.7	25.0	25.0	24.3	25.0	23.6	25.0	25.0	24.3	24.3	25.0	25.0	25.7	25.7	25.0	25.7	25.7	24.3	21.6
100.0	25.5	24.5	24.5	25.3	23.6	23.6	23.6	23.6	23.6	23.6	23.6	22.8	23.6	22.8	22.8	23.6	23.6	23.6	22.8	23.6	23.6	23.4

References

- [1] Eiji Tomita, Nobuyuki Kawahara, Zhenyu Piao and Shogo Fujita, Hydrogen Combustion and Exhaust Emissions Ignited with Diesel Oil in a Dual Fuel Engine, SAE Paper 2001-01-3503:pp. 97-102, 2001.
- [2] Naber.J.D. and Siebers.D.L, Hydrogen combustion under Diesel Engine conditions, International Journal of Hydrogen energy, Vol 23, No.5, pp. 363 –371, 1998.
- [3] N.Saravanan and G.Nagarajan, Experimental investigation in optimizing the hydrogen fuel on a hydrogen diesel dual-fuel engine, International Journal of Energy and Fuels, Volume 23, pp. 2646-2657, 2009.
- [4] Das.L.M, Fuel induction techniques for a hydrogen operated engine, Hydrogen fuel for surface transportation, Published by Society of Automotive Engineers, Inc U.S.A: pp. 27-36, 1996.
- [5] N.Saravanan and G.Nagarajan, Combustion analysis on a DI diesel engine with hydrogen in dual fuel mode, International Journal of Fuel, Volume 87, pp. 3591-3599, 2008.
- [6] James W.Heffel, Michael N. Mcclanahan, Joseph M. Norbeck, Electronic fuel injection for Hydrogen fueled Internal Combustion Engines”, University of California, Riverside, CE-CER 1998; SAE 981924, pp. 421-432, 1998.
- [7] National hydrogen energy roadmap pathway for transition to hydrogen energy for India (2007), National hydrogen energy board, Ministry of new and renewable energy and Government of India, pp.1-70.
- [8] XIth plan proposals for new and renewable energy (2006), Ministry of new and renewable energy, Government of India, pp.1-64.
- [9] L.M. Das, Near-term Introduction of Hydrogen engines for automotive and agriculture application”, Centre for energy studies, IIT, Hauz Zhas, New Delhi – 110 016, India. International Journal of Hydrogen Energy, 27, pp. 479-487, 2002.
- [10] Yi H.S., Min K. and Kim E.S. The optimized mixture formation for Hydrogen fuelled engine, International Journal of Hydrogen Energy, Vol.25, pp.685-690.
- [11] Masood M., Mehdi S.N., Omar M. and Reddy P.R., Effect of Injection delay on performance and emissions in hydrogen diesel dual fuel engine at different compression ratios, Institute of Engineers, Vol.87, pp.24-25, 2006.
- [12] Jong T. Lee. and Kim.Y.Y, The Development of a Dual Injection Hydrogen fueled engine with High power and high efficiency, Fall Technical Conference of ASME-ICED: pp.2-12, 2002.
- [13] James W. Heffel, NOX emission and performance data for a hydrogen fuelled internal combustion engine at 1500 rpm using exhaust gas recirculation, Internal Journal of Hydrogen Energy, Vol.28:pp. 901-908, 2003.
- [14] Ladommatos N., Abdelhalim S.M., Zhao H. and Hu Z, Effects of EGR on heat release in diesel combustion, SAE Transactions 980184:pp. 1-15, 1998.
- [15] N.Saravanan and G.Nagarajan, An insight on hydrogen fuel injection techniques with SCR system for NO_x reduction in a hydrogen–diesel dual fuel engine, International Journal of Hydrogen Energy, Volume 34, pp. 9019-9032, 2009.
- [16] Addison Bain and Wm D. Van vorst, The Hindenburg tragedy revisited: the fatal flaw found, International Journal of Hydrogen Energy, Vol.24, pp.399-403, 1999.
- [17] Verhelst S. and Sierens R, Aspects concerning the Optimisation of a Hydrogen Fueled Engine, International Journal of Hydrogen energy, 26: pp. 981-985, 2001.
- [18] S Verhelst, S Verstraetran and R Sierens, A comprehensive overview of hydrogen engine design features, Proceedings of the Institution of Mechanical Engineers, Part D: Journal of Automobile Engineering, Volume 221, Number 8, pp 911-920, 2007.
- [19] Holman, J. P. Experimental methods for engineers, 1973 (McGraw-Hill).
- [20] N.Saravanan and G.Nagarajan, An experimental investigation on optimized manifold injection in a direct-injection diesel engine with various hydrogen flow rates, Proceedings of the Institution of Mechanical Engineers, Part D: Journal of Automobile Engineering, Volume 221, Number 12, pp 1575-1584, 2007.
- [21] S.Singh, L Llang SC kong and RD Reitz ,Development of a Flame Propagation Model for Dual-Fuel Partially Premixed Compression Ignition Engines, International journal of Engine research, Volume 7, Number 1, pp.1468-1474, 2006.

- [22] V Pirouzpanah and R Khoshbakhti Saray, Enhancement of the combustion process in dual-fuel engines at part loads using exhaust gas recirculation, ImechE part D, Volume 221, Number 7 pp. 877-888, 2007.
- [23] S. Singh, S.R. Krishnan, K.K. Srinivasan, K.C. Midkiff and S.R. Bell, Effect of pilot injection timing, pilot quantity and intake charge conditions on performance and emissions for an advanced low-pilot-ignited natural gas engine, International journal of Engine research, Volume 5, Number 4, pp. 329-348, 2004.
- [24] K K Srinivasan, S R Krishnan and K C Midkiff, Improving low load combustion, stability, and emissions in pilot-ignited natural gas engines , ImechE part D, Volume 220, Number 2, pp. 229-239, 2006.



N.Saravanan, M.E, PhD ongoing in Hydrogen combustion in Diesel engine systems. He is having research interest in Alternative fuels, engine calibration, emission optimization. Mr. N.Saravanan is member of SAE, ISTE.

E-mail address: sarav_2003@yahoo.co.in, saravanan.n@tatamotors.com



G.Nagarajan, M.E, PhD. He is having research interest in the area of alternative fuels for diesel engines and pollution control from I.C engines. Dr.G.Nagarajan is member of SAE, Combustion Institute (USA), ISTE, ISME and QCFI. He is also the Faculty Adviser of SAEINDIA Collegiate Club of College of Engineering.

Email address: nagarajan1963@yahoo.com